J. Micropalaeontology, 37, 105–138, 2018
https://doi.org/10.5194/jm-37-105-2018

Journal of Micropalaeontology
Open Access

Stratigraphic calibration of Oligocene–Miocene organic-walled dinoflagellate cysts from offshore Wilkes Land, East Antarctica, and a zonation proposal

Peter K. Bijl[1], Alexander J. P. Houben[2], Anja Bruls[1], Jörg Pross[3], and Francesca Sangiorgi[1]

[1]Marine Palynology and Paleoceanography, Laboratory of Palaeobotany and Palynology, Department of Earth Sciences, Faculty of Geosciences, Utrecht University, P.O. Box 80.115, 3508 TC Utrecht, the Netherlands
[2]Applied Geosciences Team, Netherlands Organisation for Applied Scientific Research (TNO), Princetonlaan 6, 3584 CB, Utrecht, the Netherlands
[3]Paleoenvironmental Dynamics Group, Institute of Earth Sciences, University of Heidelberg, Im Neuenheimer Feld 234, 69120 Heidelberg, Germany

Correspondence: Peter K. Bijl (p.k.bijl@uu.nl)

Received: 27 June 2017 – Revised: 17 October 2017 – Accepted: 21 October 2017 – Published: 5 January 2018

Abstract. There is growing interest in the scientific community in reconstructing the paleoceanography of the Southern Ocean during the Oligocene–Miocene because these time intervals experienced atmospheric CO_2 concentrations with relevance to our future. However, it has remained notoriously difficult to put the sedimentary archives used in these efforts into a temporal framework. This is at least partially due to the fact that the bioevents recorded in organic-walled dinoflagellate cysts (dinocysts), which often represent the only microfossil group preserved, have not yet been calibrated to the international timescale. Here we present dinocyst ranges from Oligocene–Miocene sediments drilled offshore the Wilkes Land continental margin, East Antarctica (Integrated Ocean Drilling Program (IODP) Hole U1356A). In addition, we apply statistical means to test a priori assumptions about whether the recorded taxa were deposited in situ or were reworked from older strata. Moreover, we describe two new dinocyst species, *Selenopemphix brinkhuisii* sp. nov. and *Lejeunecysta adeliensis* sp. nov., which are identified as important markers for regional stratigraphic analysis. Finally, we calibrate all identified dinocyst events to the international timescale using independent age control from calcareous nanoplankton and magnetostratigraphy from IODP Hole U1356A, and we propose a provisional dinoflagellate cyst zonation scheme for the Oligocene–Miocene of the Southern Ocean.

1 Introduction

There is a growing need to better understand the dynamics of the Antarctic cryosphere and the paleoceanography of the Southern Ocean during the Oligocene and Miocene, particularly in view of the apparent similarity between Oligocene and Miocene atmospheric CO_2 concentrations and those of the near future (e.g. Zhang et al., 2013). The vast majority of our understanding of Oligocene–Miocene ice-sheet dynamics and paleoceanography in the high southern latitudes is derived from marine sedimentary archives. A major challenge when employing these archives is to establish accurate age control. Many sedimentary successions from the Southern Ocean lack the calcareous microfossil groups conventionally used for biostratigraphic age control, which stresses the need to utilise the stratigraphic potential of non-calcareous microfossils. Siliceous microfossils have provided an excellent stratigraphic framework for the Neogene of the Southern Ocean (Cody et al., 2008); however, they are prone to dissolution when buried below the diagenetic front of opal, which tends to limit their applicability to deeply buried strata (DeMaster, 2003).

For successions from the southern high latitudes, organic microfossils have repeatedly been shown to represent a use-

ful biostratigraphic tool (e.g. Brinkhuis et al., 2003a, b; Sluijs et al., 2006; Tauxe et al., 2012; Pross et al., 2012; Houben et al., 2011, 2013; Stocchi et al., 2013). Recently, a calibration of Paleocene and Eocene dinocyst origination and extinction events to the geomagnetic polarity timescale (GPTS) has provided the potential for improved age control in the Southern Ocean for this part of the stratigraphic column (Bijl et al., 2013b, 2014). In contrast, a proper magnetostratigraphic calibration of organic microfossil events in the Southern Ocean for the Oligocene and Miocene epochs is still missing. This may be partially ascribed to the fact that Oligocene–Neogene dinocyst assemblages from the Southern Ocean (i) are of relatively low diversity, (ii) are dominated by stratigraphically long-ranging species (Escutia et al., 2011), (iii) contain a considerable number of formally un-described taxa (Escutia et al., 2011), and (iv) include endemic species that are highly specialised to the (paleo)oceanographic conditions prevailing around Antarctica (Houben et al., 2013). The latter means that the distribution of many dinocyst taxa found in Southern Ocean sediments is restricted to that region (e.g. Zonneveld et al., 2013; Houben et al., 2013). These typical Southern Ocean assemblages were essentially established during the Eocene–Oligocene transition, in conjunction with the onset of major Antarctic cryosphere growth (Houben et al., 2013). As a consequence of the abovementioned characteristics, these dinoflagellate cyst assemblages have yet yielded virtually no bio-events that could be calibrated to the internationally used geologic timescale (Gradstein et al., 2012).

Studies on Oligocene–Neogene dinocyst assemblages have been carried out on sediment cores from Prydz Bay (Hannah, 2006; Warnaar, 2006; Houben et al., 2013), Cape Roberts (Hannah et al., 1998, 2000, 2001a, b), within the Cenozoic Investigation in the Western Ross Sea (CIROS) program (Hannah, 1994, 1997), the Antarctic Geological Drilling (ANDRILL) program in the Ross Sea (Warny et al., 2009), and Ocean Drilling Program (ODP) Site 696 in the Weddell Sea (Warnaar, 2006; Houben et al., 2013). Further north in the Southern Ocean, dinocyst records have been generated from ODP Site 1168 (Brinkhuis et al., 2003a) and Deep Sea Drilling Project (DSDP) Site 511 (Goodman and Ford Jr., 1983; Houben et al., 2011). Efforts to accurately calibrate the dinocyst events encountered in these studies to existing timescales were not only hindered by taxonomical challenges, but also by other factors such as a lack of independent age control or relatively short and/or incomplete sedimentary archives. A recent revisit of sedimentary records from the Cape Roberts Project (CRP) has yielded formal descriptions of a number of dinocyst species, the ranges of which have been stratigraphically calibrated to some extent (Clowes et al., 2016).

Clearly, a proper stratigraphic calibration of Oligocene–Miocene dinocyst events in the Southern Ocean could provide age constraints for many sedimentary records that have yet remained stratigraphically poorly dated and would also provide an opportunity to date sediments to be recovered

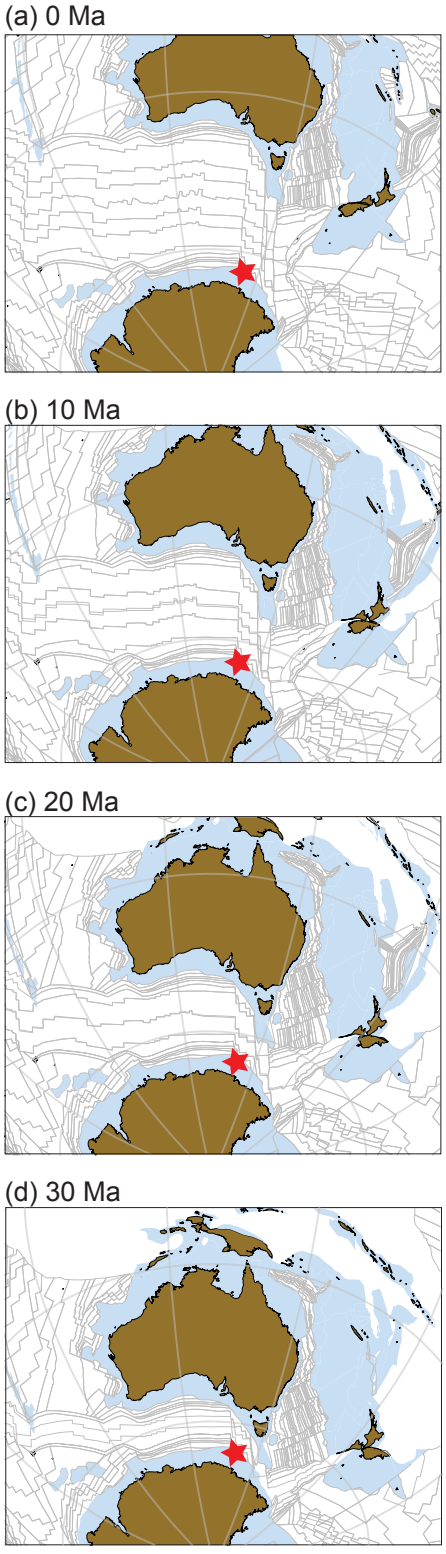

Figure 1. Paleogeography of the southwestern Pacific Ocean and position of IODP Site U1356 (red star) at **(a)** 0 Ma, **(b)** 10 Ma, **(c)** 20 Ma and **(d)** 30 Ma. Figures adapted from G plates, with plate circuit from Seton et al. (2012) and absolute plate positions of Torsvik et al. (2012).

during future drilling campaigns (e.g. McKay et al., 2016). In 2010, IODP Expedition 318 drilled a series of sedimentary archives off the Wilkes Land margin, East Antarctica (notably Site U1356; Fig. 1). In this paper, we present and describe dinocysts encountered in the Oligocene and Miocene part of the succession at Site U1356, with the aim of tying their distribution to the existing integrated bio-magnetostratigraphic age model (Tauxe et al., 2012). We critically evaluate the likelihood that certain species are reworked from older strata or deposited in situ using multivariate statistical analysis. We formally describe two new species, which we consider stratigraphically useful, while we informally report 23 other new taxa. Finally, we establish a first dinocyst zonation scheme for the Oligocene–Miocene of the Southern Ocean.

2 Material

2.1 Site description and lithology of IODP Hole U1356A

This research uses samples from IODP Hole U1356A, which was drilled on the base of the continental rise of the Wilkes Land continental margin (Fig. 1a; present latitude 63°18.6′ S, 135°59.9′ E; Escutia et al., 2011). From early Oligocene (∼ 34 Ma) to middle Miocene (∼ 10 Ma) times, the site has moved from a paleolatitude of 59.8 ± 4.8° to 61.5 ± 3.3° S respectively (Van Hinsbergen et al., 2015; Fig. 1). Oligocene and Miocene sediments were recovered between 890 and 3 m below sea floor (m b.s.f.; Fig. 2). Core recovery was poor for the uppermost 95 m of Hole U1356A, as a consequence we focus our analyses on the interval between 95.4 and 894 m b.s.f. (Cores 11R to 95R Section 3).

Sediments consist of alternations of laminated and bioturbated siltstones, occasional claystones and coarser beds, the latter of which are occasionally deformed. Such deposits indicate contourite deposition (Escutia et al., 2011). Occasionally, carbonate is so abundantly present that limestone beds were formed. Diatoms are abundant down-core to about 400 m b.s.f. but are not preserved below this level. The presence of calcareous nanoplankton indicates that the carbonates were derived from a pelagic, biogenic source. Outsized clasts are confined to specific depth intervals. These intervals are 890–875, 735–675, 580–450 and 200–150 m b.s.f. (Escutia et al., 2011).

2.2 Bio-magnetostratigraphic age model for IODP Hole U1356A

Stratigraphic constraints for the Oligocene–Miocene succession from IODP Hole U1356A comprise calcareous nanoplankton, radiolarian, diatom, sparse dinocyst biostratigraphy and magnetostratigraphy (Tauxe et al., 2012; Fig. 2). The work of Tauxe et al. (2012) was calibrated to the Gradstein et al. (2004) timescale. Here we update the age model of the succession to the GPTS of Gradstein

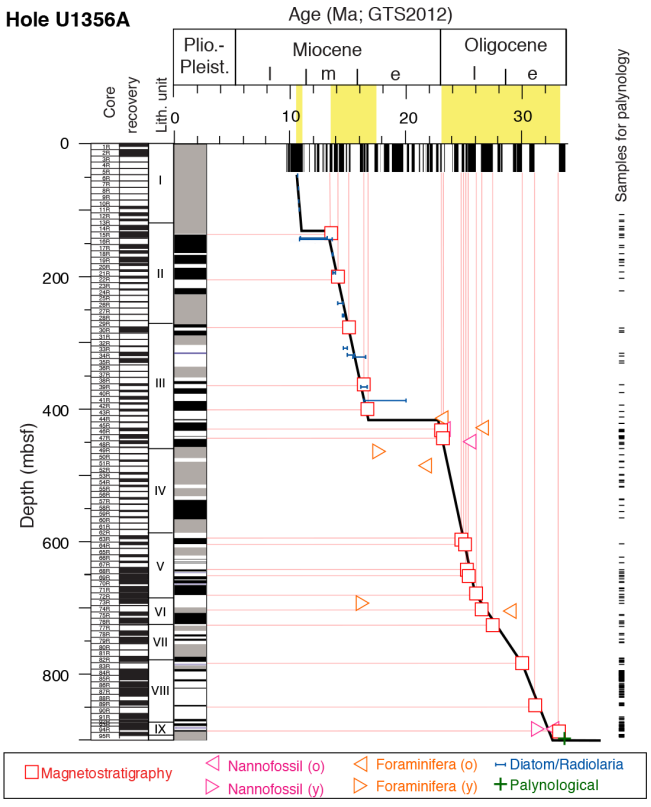

Figure 2. Integrated Ocean Drilling Program Hole U1356A. Core recovery, lithostratigraphic units, age–depth plot and position of samples taken for palynology. Palaeomagnetic data were obtained from Tauxe et al. (2012), in which black is normal polarity, white is reversed, lilac is uncertain polarity and grey is no data. Age model has been (re-)calibrated to GTS2012 of Gradstein et al. (2012); see text and Table 1.

et al. (2012; Table 1). Furthermore, the age model for the Miocene part of the succession had been updated by Crampton et al. (2016) using constrained optimisation of available stratigraphic datums (CONOP; see also Sangiorgi et al., 2017); here we follow this updated age model for the Miocene part of the succession.

These revisions suggest that the sediments between 895.4 and 95.4 m b.s.f. (i.e. Cores U1356A-95R-3w, 82 cm to U1356A-11R) were deposited between the earliest Oligocene (33.7 Ma) and early late Miocene (10.7 Ma). A 14 Myr long hiatus at 895.4 m b.s.f. spans the mid-Eocene to earliest Oligocene (46–33.7 Myr). Crampton et al. (2016) identified a hiatus between Cores 14R and 15R that was previously unaccounted for. Tauxe et al. (2012) interpreted a hiatus between Cores 46R and 47R, lasting from ∼ 23.0 to 17.0 Ma. Above Core 45R, high-resolution diatom biostratigraphy suggests that the succession is nearly continuous (Tauxe et al., 2012). However, Cores 45R-47R yield insufficient stratigraphic information to confidently assign an age. Our study presents high-resolution dinocyst data, identification of new stratigraphic markers and a revisit of the exist-

Table 1. Age constraints for the Oligocene–Miocene of Hole U1356A. Ages printed in bold are adjusted relative to the information given in Tauxe et al. (2012).

Type	FO/LO	Genus, chron	Species	Age (Gradstein et al., 2012)	Top core	Top interval	Bottom core	Bottom interval	Depth average	Error
R	FO	*Helotholus*	*vema*	**4.20**	Hole top		1R-1,	3–5	0.03	0.03
D	LO	*Rouxia*	*peragalli*	**4.67**	Hole top		1R-1,	3–5	0.03	0.03
D	FO	*Thalassiosira*	*inura*	**5.07**	1R-2,	138–139	1R	CC	3.67	0.79
D	FO	*Thalassiosira*	*oliverana*	**6.62**	1R-2,	138–139	1R	CC	3.67	0.79
D	FO	*Rouxia*	*peragalli*	**7.00**	1R-1,	3–5	1R	CC	2.25	2.22
D	FO	*Fragilariopsis*	*clementia*	**7.03**	1R-1,	3–5	1R	CC	2.25	2.22
D	FO	*Rouxia*	*californica*	**8.62**	1R-1,	3–5	1R	CC	2.25	2.22
D	LO	*Denticulopsis*	*simonsenii*	**8.66**	Hole	top	1R-1,	3–5	0.03	0.03
D	FO	*Thalassiosira*	*torokina*	**9.16**	1R-2,	138–139	1R	CC	3.67	0.79
D	LO	*Denticulopsis*	*ovata*	**9.64**	3R-CC		4R-CC		24.09	4.29
D	FO	*Thalassiothrix*	*miocenica*	**10.14**	4R-CC		**6R-CC**		37.80	9.51
D	LO	*Denticulopsis*	*dimorpha* var. *areolata*	**10.25**	3R-CC		4R-CC		24.09	4.29
D	FO	*Denticulopsis*	*dimorpha* var. *areolata*	**10.31**	7R-CC		9R-CC		66.50	9.60
R	LO	*Cycladophora*	*humerus*	**10.41**	1R-CC		3R-CC		12.20	7.60
D	FO	*Eucampia*	*antarctica*	**10.46**	28R-CC		29R-CC		263.20	4.80
D	LO	*Denticulopsis*	*dimorpha*	**10.66**	3R-CC		4R-CC		24.09	4.29
D	FO	*Denticulopsis*	*ovata*	**11.10**	6R-CC		7R-CC		52.10	4.80
D	FO	*Denticulopsis*	*dimorpha*	**12.20**	8R-CC		9R-CC		71.30	4.80
R	FO	*Cycladophoa*	*spongothrax*	**12.70**	10R-CC		12R-CC		97.44	11.74
D	FO	*Denticulopsis*	*praedimorpha*	**12.86**	8R-CC		16R-CC		104.95	38.45
PM	(y)	C5AB		**13.36**	14R-5,	80	15R-1,	10	132.15	1.75
PL	FO	*Selenopemphix*	*dioneacysta*	**13.40**	15R-6,	20–22	17R-1,	20–22	147.10	6.10
D	FO	*Nitzschia*	*denticuloides*	**13.59**	21R-CC		22R-CC		198.74	5.08
R	FO	*Actinomma*	*golowini*	**13.66**	14R-CC		15R-CC		136.00	5.53
PM	(o)	C5ACn		**14.07**	22R-2,	75	22R-2,	90	203.23	0.07
D	LO	*Denticulopsis*	*maccollumii*	**14.20**	24R-CC		25R-CC		226.01	3.94
R	FO	*Cycladophora*	*humerus*	**14.24**	21R-CC		22R-CC		198.74	5.08
D	FO	*Denticulopsis*	*simonsenii*	**14.29**	23R-CC		24R-CC		216.87	5.03
D	FO	*Actinocyclus*	*ingens* var. *nodus*	**14.47**	28R-CC		29R-CC		263.20	4.80
D	LO	*Cavitatus*	*jouseanus*	**14.66**	34R-CC		35R-CC		326.33	5.16
PM	(y)	C5Bn.2n		**15.03**	30R-2,	50	30R-2,	75	279.63	0.13
D	FO	*Denticulopsis*	*lauta*	**15.78**	31R-CC		33R-CC		297.19	10.19
PM	(o)	C5Cn.1n		**16.27**	39R-1,	35	39R-1,	65	364.10	0.15
PM	(o)	C5Cn.3n		**16.72**	42R-2,	59	43R-1,	25	398.28	3.98
D	FO	*Denticulopsis*	*maccollumii*	**16.95**	41R-CC		**42R-2,**	**59**	390.59	3.71
R	FO	*Eucyrtidium*	*punctatum*	**17.00**	41R-CC		**42R-2,**	**59**	390.59	3.71
D	FO	*Actinocyclus*	*ingens*	**17.52**	38R-CC		41R-CC		370.37	16.37
F	LO	*Catapsydrax*	*dissimilis*	**17.59**	**49R-CC**		50R-CC		464.93	4.85
PL	FO	*Pyxidinopsis*	*fairhavenensis*	**21.00**	44R-1,	20–22	45R-1,	10–14	416.57	4.76
F	FO	*Globigerina*	*connecta*	**21.50**	50R-CC		**53R-CC**		485.01	15.23
F	LO	*Globigerina*	*euapertura*	**23.03**	**43R-CC**		45R-CC		413.53	8.66
PM	(o)	C6Cn.2n		**23.03**	45R-CC	40	46R-1	65	426.78	5.00
PL	FAO	*Invertocysta*	*tabulata*	**23.03**	55R-1,	18–20	55R-2,	18–20	479.53	0.75
CN	LO	*Reticulofenestra*	*bisecta*	**23.13**	46R-1,	68–72	46R-1,	119–123	431.74	0.25
PM	(o)	C6Cn.3n		**23.30**	50R-1,	0			469.00	9.00
PM	(y)	C7An		**24.76**	63R-3,	85	63R-3,	120	597.12	0.17
PM	(o)	C7An		**24.98**	64R-1,	130	64R-1,	135	604.33	0.02
PM	(o)	C8n.1n		**25.26**	68R-2,	20	68R-2,	75	643.38	0.27
PM	(y)	C8n.2n		**25.30**	69R-2,	20	69R-2,	25	652.58	0.02
CN	LO	*Chiasmolithus*	*altus*	**25.44**	48R-1,	6–7	48R-1,	16–17	450.01	0.05
PM	(o)	C8n.2n		**25.99**	71R-6,	115	72R-1,	10	678.98	0.92
PM	(y)	C9n		**26.42**	73R-4,	90	75R-1,	15	701.66	7.09
F	LO	*Globobiergina*	*labiacrassata*	**26.52**	**45R-CC**		46R-CC		428.40	6.21
PM	(o)	C9n		**27.44**	76R-6,	35	76R-6,	40	725.09	0.02
F	FO	*Rectuvigerina*	*stonei*	**28.85**	73R-CC		**75R-CC**		704.65	9.29
PM	(o)	C11n.2n		**29.97**	82R-6,	35	82R-6,	40	782.68	0.03
CN	LO	*Reticulofenestra*	*umbilicus*	**31.30**	93R-CC		94R-4,	29–30	883.34	2.59
CN	LO	*Isthmolithus*	*recurvus*	**32.49**	93R-CC		94R-4,	29–30	883.34	2.59
PM	(y)	C13n		**33.16**	93R-1,	117	93R-2,	28	878.00	0.23
PL	FO	*Malvinia*	*escutiana*	**33.50**	95R-3,	82–85	95R-3,	106–109	894.80	0.12

Table 2. List of dinocyst species and their PCA scores. **(a)** Species assumed in situ; **(b)** species assumed reworked. Taxonomy according to that cited in Williams et al. (2017). Eigenvalues and cumulative % explained by the axes are indicated.

(a) Assumed in situ species name	*n*	PCA axis 1	PCA axis 2	PCA axis 3	PCA axis 4	Positive on first two axes
Eigenvalues		0.299	0.172	0.086	0.069	
Cumulative % variance of species data		29.856	47.025	55.622	62.501	
Adnatosphaeridium? sp.	10	0.047	−0.051	−0.024	−0.024	n
Ataxodinium choane	41	0.134	−0.101	−0.095	−0.056	n
Batiacasphaera compta	3	0.033	0.095	0.018	0.024	y
Batiacasphaera spp. (pars.)	94	−0.238	−0.018	0.450	−0.061	n
Batiacasphaera hirsuta	29	0.121	−0.149	−0.142	−0.079	n
Batiacasphaera micropapillata	24	0.150	−0.178	−0.104	0.514	n
Batiacasphaera minuta	132	0.259	−0.363	−0.391	−0.083	n
Batiacasphaera sphaerica	46	0.203	−0.247	−0.158	0.022	n
Batiacasphaera sp. A	66	−0.132	−0.074	0.138	0.199	n
Batiacasphaera sp. B	21	−0.040	−0.024	0.250	−0.066	n
Batiacasphaera sp. C	109	0.017	−0.318	0.648	−0.431	n
Batiacasphaera sp. D	5	0.009	0.033	−0.036	−0.025	y
Brigantedinium pynei	119	0.170	−0.322	−0.563	−0.517	n
Brigantedinium simplex	10 763	−8.098	2.641	−5.230	0.712	n
Brigantedinium sp. A	251	−0.941	0.078	−1.521	0.363	n
Brigantedinium sp. B	37	0.030	−0.054	−0.161	−0.215	n
Brigantedinium sp. C	2	0.003	−0.005	−0.030	−0.028	n
Brigantedinium sp. D	29	0.029	−0.053	−0.198	−0.217	n
Cerebrocysta delicata	11	−0.019	−0.001	0.165	−0.049	n
Cerebrocysta sp. A	183	0.508	−0.832	−0.053	2.313	n
Cerebrocysta sp. B	37	0.163	−0.192	0.113	0.638	n
Cleistosphaeridium sp. B	2	−0.006	−0.006	0.054	0.006	n
Cleistosphaeridium sp. A	386	1.133	3.178	0.498	0.411	y
Cordosphaeridium minutum	46	0.061	−0.081	−0.100	−0.111	n
Corrudinium labradori	831	−2.128	0.085	0.258	0.958	n
Corrudinium sp. A	19	−0.186	−0.006	0.425	0.202	n
Cryodinium? sp.	2	0.008	−0.012	−0.022	−0.035	n
Distatodinium spp.	1	0.007	−0.004	−0.012	−0.017	n
Edwardsiella sexispinosa	2	0.017	−0.023	−0.016	0.094	n
Elytrocysta brevis	58	−0.057	0.327	0.314	0.194	n
Elytrocysta sp. A	85	−0.046	0.391	−0.006	0.046	n
Gelatia inflata	161	−0.735	0.083	0.578	0.280	n
Habibacysta? spp.	5	0.029	−0.047	−0.045	0.047	n
Homotryblium spp.	13	0.053	0.105	0.025	−0.012	y
Hystrichosphaeropsis obscura	2	0.017	−0.018	−0.004	−0.002	n
Hystrichokolpoma bullatum	34	−0.214	−0.006	0.507	0.204	n
Impagidinium aculeatum	160	0.202	−0.687	0.027	2.276	n
Impagidinium cantabrigiense	48	0.287	−0.383	−0.148	1.360	n
Impagidinium elegans	31	0.201	0.626	0.107	0.122	y
Impagidinium elongatum	4	0.025	−0.025	−0.007	0.014	n
Impagidinium japonicum	1	0.007	−0.004	−0.012	−0.017	n
Impagidinium pallidum	515	1.264	−1.747	−0.312	3.677	n
Impagidinium paradoxum	267	1.049	0.226	−0.472	3.010	y
Impagidinium patulum	144	0.351	0.127	−0.400	0.365	y
Impagidinium plicatum	17	0.052	−0.051	−0.014	0.029	n
Impagidinium velorum	75	−0.150	−0.110	0.267	0.380	n
Impagidinium victorianum	381	−0.735	0.868	0.419	2.070	n
Impagidinium sp. A	14	0.021	−0.053	0.155	−0.174	n
Impagidinium sphaericum	1	0.011	−0.010	−0.002	−0.019	n
Impagidinium spp. (pars.)	93	0.441	−0.581	−0.277	1.048	n
Invertocysta tabulata	72	0.392	−0.535	−0.104	1.675	n
Islandinium spp.	38	0.106	−0.127	−0.175	−0.296	n
Lejeunecysta attenuata	72	−0.463	−0.043	0.251	0.197	n
Lejeunecysta adeliensis sp. nov.	304	0.291	1.587	−1.139	−0.082	y
Lejeunecysta fallax	5059	−6.987	0.933	2.429	2.861	n
Lejeunecysta cowei	9	0.034	−0.049	−0.093	−0.078	n
Lejeunecysta acuminata	710	−2.156	1.016	−1.440	0.667	n
Lejeunecysta rotunda	175	−0.782	0.797	−1.267	0.382	n

Table 2. Continued.

(a) Assumed in situ species name	*n*	PCA axis 1	PCA axis 2	PCA axis 3	PCA axis 4	Positive on first two axes
Lejeunecysta katatonos	224	−1.359	0.095	0.292	0.673	n
Malvinia escutiana	864	−0.593	2.836	−0.906	0.769	n
Nematosphaeropsis labyrinthus	1234	1.307	−2.573	0.052	7.758	n
Oligokolpoma galeotti	7	−0.080	0.021	−0.114	0.062	n
Operculodinium cf. *eirikianum*	162	−0.009	−0.567	0.949	1.642	n
Operculodinium tiara	97	−0.111	−0.070	0.057	−0.183	n
Operculodinium eirikianum	340	−0.563	−0.609	0.635	0.474	n
Operculodinium janduchenei	88	0.200	−0.365	0.258	0.262	n
Operculodinium piaseckii	158	0.561	−0.821	−0.495	2.654	n
Operculodinium sp. A	164	0.550	−0.649	−0.240	0.483	n
Paleocystodinium golzowense	12	0.034	0.022	−0.019	−0.059	y
Paucisphaeridium spp.	20	−0.163	0.005	0.362	0.113	n
Phthanoperidinium amoenum	4	−0.011	0.032	0.040	0.033	n
Protoperidinioid indet	274	0.262	−0.385	−0.605	−1.032	n
Protoperidinium sp. A	2699	−0.223	0.293	−0.312	−0.102	n
Protoperidinium sp. B	111	−2.856	−1.148	10.091	−1.256	n
Protoperidinium sp. C	14	−0.026	0.006	0.032	0.004	n
Protoperidinium sp. D	105	0.009	−0.030	−0.259	−0.681	n
Pyxidinopsis fairhavenensis	31	0.129	−0.138	−0.117	−0.168	n
Pyxidinopsis reticulata	20	0.107	−0.113	−0.066	−0.050	n
Pyxidinopsis sp. A	25	−0.040	−0.106	0.218	0.109	n
Pyxidinopsis sp. B	6	−0.058	0.007	0.135	0.051	n
Pyxidinopsis sp. C	14	0.134	−0.170	−0.045	0.647	n
Pyxidinopsis sp. D	21	0.149	−0.202	−0.079	0.846	n
Pyxidinopsis spp. (pars.)	352	0.112	−0.841	0.177	3.222	n
Pyxidinopsis tuberculata	247	0.708	−1.000	−0.496	3.489	n
Pyxidinopsis vesciculata	28	0.157	−0.182	−0.119	0.005	n
Reticulatosphaera actinocoronata	24	0.078	0.270	−0.172	0.250	y
Selenopemphix brinkhuisii sp. nov.	456	−1.988	0.190	0.164	1.040	n
Selenopemphix antarctica	477	−0.133	1.110	−1.521	−0.428	n
Selenopemphix dioneacysta	2	0.009	−0.007	−0.005	−0.013	n
Selenopemphix nephroides	1223	−2.365	0.117	1.461	−0.059	n
Selenopemphix sp. A	2	0.008	−0.009	−0.018	−0.018	n
Selenopemphix undulata	6	0.006	−0.031	−0.079	0.017	n
Spiniferites sp. A	3	−0.008	0.034	0.094	0.028	n
Spiniferites sp. B	4	−0.007	−0.019	0.077	−0.032	n
Spiniferites sp. C	4	0.019	−0.017	0.021	−0.022	n
Stoveracysta kakanuiensis	5	0.041	0.143	−0.001	0.033	y
Stoveracysta ornata	18	−0.172	−0.012	0.449	0.119	n
?*Svalbardella* spp.	3	−0.008	−0.004	−0.001	0.012	n
Tectatodinium spp.	4	−0.001	0.039	0.065	0.000	n
Unipontidinium aquaeductum	6	0.042	−0.042	−0.003	0.020	n
(b) Assumed reworked species name	*n*	PCA axis 1	PCA axis 2	PCA axis 3	PCA axis 4	Positive on first two axes
Eigenvalues		0.299	0.172	0.086	0.069	
Cumulative % variance of species data		29.856	47.025	55.622	62.501	
Achilleodinium biformoides	1	0.014	0.034	0.024	0.008	y
Achomosphaera alcicornu	26	0.058	0.298	0.259	0.091	y
Adnatosphaeridium spp.	21	0.166	0.429	0.090	−0.006	y
Aiora fenestrata	3	0.037	0.018	0.001	0.080	y
Aireiana verrucosa	1	0.017	0.053	0.018	0.011	y
Alisocysta circumtabulata	1	−0.011	0.003	−0.026	0.003	n
Alterbidinium distinctum	21	0.154	0.410	0.124	0.158	y
Apectodinium spp.	6	0.069	0.151	0.039	0.004	y
Arachnodinium antarcticum	52	0.296	0.918	0.158	0.243	y
Areoligera spp. (pars.)	8	0.047	0.132	0.087	0.011	y
Areoligera semicirculata	1	0.014	0.034	0.024	0.008	y
Cerebrocysta bartonensis	97	0.436	1.351	0.272	0.302	y
Charlesdowniea clathrata	2	0.028	0.023	0.002	0.085	y
Charlesdowniea edwardsii	19	0.099	0.221	0.033	0.025	y

Table 2. Continued.

(b) Assumed reworked species name	*n*	PCA axis 1	PCA axis 2	PCA axis 3	PCA axis 4	Positive on first two axes
Cooksonidinium capricornum	1	0.011	0.032	0.005	0.016	y
Cordosphaeridium fibrospinosum	116	0.541	1.439	0.430	0.193	y
Cordosphaeridium furniculatum	1	−0.012	−0.002	0.020	0.005	n
Corrudinium incompositum	13	0.081	0.309	−0.062	0.083	y
Corrudinium regulare	9	0.061	0.120	0.056	0.025	y
Cribroperidinium spp.	21	0.144	0.404	0.125	0.062	y
Damassadinium crassimuratum	2	0.027	0.046	0.021	−0.004	y
Dapsilidinium spp.	9	−0.012	0.059	0.043	0.048	n
Deflandrea antarctica	546	−0.375	0.995	2.063	1.351	n
Deflandrea cygniformis	5	0.040	0.118	0.036	0.034	y
Deflandrea sp. A sensu Brinkhuis et al. 2003b	16	0.024	0.163	0.145	0.038	y
Deflandrea spp. indet	1805	2.402	6.988	0.886	0.916	y
Diphyes colligerum	1	−0.011	−0.002	0.040	0.017	n
Eisenackia circumtabulata	2	0.002	0.040	0.009	0.014	y
Enneadocysta dictyostila	1838	−0.371	2.711	1.821	2.471	n
Enneadocysta multicornuta	24	−0.045	0.172	−0.045	0.074	n
Eocladopyxis tesselata	11	0.060	0.256	0.100	0.036	y
Fibrocysta axialis	5	0.060	0.154	0.029	0.005	y
Glaphyrocysta intricata	4	0.035	0.101	0.015	0.030	y
Glaphyrocysta pastielsii	249	0.737	2.000	0.481	0.265	y
Heteraulacacysta leptalea	4	0.015	0.057	0.059	−0.016	y
Histiocysta palla	2	0.001	−0.002	0.017	−0.019	n
Hystrichokolpoma pusilla	2	0.020	0.066	0.006	0.027	y
Hystrichokolpoma rigaudiae	5	0.054	0.112	0.061	0.000	y
Hystrichokolpoma truncatum	24	0.191	0.502	0.118	0.063	y
Hystrichosphaeridium truswelliae	78	0.431	1.228	0.278	0.201	y
Hystrichosphaeridium tubiferum	2	0.010	0.034	0.021	−0.006	y
Impagidinium maculatum	20	0.171	0.540	0.052	0.116	y
Kenleyia spp.	4	0.039	0.108	0.026	0.021	y
Manumiella druggii	3	−0.001	−0.010	−0.018	−0.009	n
Melitasphaeridium pseudorecurvatum	2	0.031	0.056	0.023	−0.004	y
Membranophoridium perforatum	48	0.355	0.993	0.197	0.200	y
Octodinium askiniae	20	0.145	0.357	0.105	0.056	y
Odontochitina spp.	16	−0.082	0.028	0.033	0.029	n
Operculodinium spp.	267	0.634	2.217	−0.387	0.400	y
Phthanoperidinium antarcticum	17	0.051	0.229	−0.087	0.078	y
Phthanoperidinium stockmansii	153	0.633	1.566	0.423	0.135	y
Polysphaeridium spp.	17	0.149	0.384	0.094	0.042	y
Rhombodinium sp.	2	0.030	0.066	0.034	0.001	y
Schematophora speciosa	4	0.016	0.058	0.017	0.017	y
Schematophora obscura	4	0.049	0.128	0.020	0.018	y
Senegalinium spp.	117	0.418	1.399	0.067	0.178	y
Spinidinium luciae	2	0.027	0.046	0.021	−0.004	y
Spinidinium macmurdoense	62	0.242	0.842	0.314	0.393	y
Spinidinium schellenbergii	17	−0.020	0.215	0.106	0.096	n
Spiniferites ramosus CPX	1008	1.760	4.444	1.326	1.526	y
Thalassiphora pelagica	9	0.000	0.160	0.158	0.069	y
Turbiosphaera filosa	8	0.068	0.227	0.013	0.049	y
Turbiosphaera sagena	14	0.105	0.311	0.058	0.066	y
Vozzhennikovia apertura/ S.schellenbergii group	834	0.977	4.131	1.505	0.828	y
Vozzhennikovia netrona	14	0.008	0.028	0.156	−0.040	y
?*Vozzhennikovia* LARGE	2	0.026	0.065	0.022	0.008	y
Wetzeliella articulata	3	0.035	0.077	0.033	0.001	y
Ynezidinium waipawaense	6	0.070	0.118	0.021	−0.022	y

ing carbonate microfossil data, which shed new light on the Oligocene–Miocene boundary interval. Although we interpolate sedimentation rates linearly between our stratigraphic tie points, the depositional setting and the incomplete recovery for Hole U1356A dictates caution in inferring continuous sedimentation throughout the record.

3 Methods

3.1 Palynological sample processing

In total, 272 samples were processed and studied for palynology. Sample resolution varies between 20 cm in Core 84R-

85R to over 9 m in intervals of low core recovery (Fig. 2). Palynological processing of freeze-dried, crushed and weighed samples (13 g on average, with a standard deviation of 3.4 g) involved decalcification overnight with 30 % hydrochloric acid (HCl), followed by decanting, rinsing with water and centrifuging (2100 rotations per minute (rpm) for 5 min). The decanted residue was further processed by adding 38 % hydrofluoric acid (HF) to remove silicates. After completion of the chemical reaction with HF, samples were placed on a shaker table for about 2 h, and subsequently were allowed to settle overnight. An excess of 30 % HCl was added to remove fluoride gels, after which samples were centrifuged (2100 rpm for 5 min) and decanted. The entire HF step was repeated for full digestion of silicates. Organic residues were sieved over a 250 µm sieve to remove large palynoclasts, and the supernatant was sieved over a 10 µm sieve, with help of an ultrasonic bath to break and clean up organic residue. The remaining residues were mounted on glass microscope slides with glycerine jelly, and cover slips were sealed with nail polish. All palynological residues and microscope slides are stored in the collection of the Laboratory of Palaeobotany and Palynology of Utrecht University, the Netherlands.

3.2 Taxonomy and nomenclature

Dinoflagellate cyst taxonomy follows that cited in Williams et al. (2017; available through AASP – The Palynological Society at http://www.palynology.org and as a website at http://dinoflaj.smu.ca/dinoflaj3/), with the exception of the taxonomy of the subfamily Wetzelielloideae, for which we follow Bijl et al. (2016; see Table 2 for a species list). Of particular stratigraphic importance are the numerous species and morphotypes of the genus *Lejeunecysta* encountered, many of which have recently been formally described from Cape Roberts, Ross Sea (Clowes et al., 2016). At least 25 new dinocyst taxa were recognised in our study, two of which we consider key species for stratigraphy and formally describe herein. The remaining 23 species are informally described (Table 3). The nomenclature of dinocyst features follows Evitt (1985).

3.3 Statistical approach for defining reworked versus in situ dinocysts

A prominent feature in the palynological associations from the Oligocene and Miocene of IODP Site U1356 is the abundance of dinocysts that were initially assumed reworked from older strata. Reworked Eocene taxa dominate the palynological assemblages in the lowermost 30 m of the Oligocene (Cores 95R to 93R; Houben et al., 2013). In the lower Oligocene, the percentage of reworked elements decreases to around 10–15 % of the total palynomorph count (Houben et al., 2013). Dinocyst studies of Oligocene and younger sediments in the circum-Antarctic area are scarce, which makes the assumption that certain taxa recorded in the Oligocene

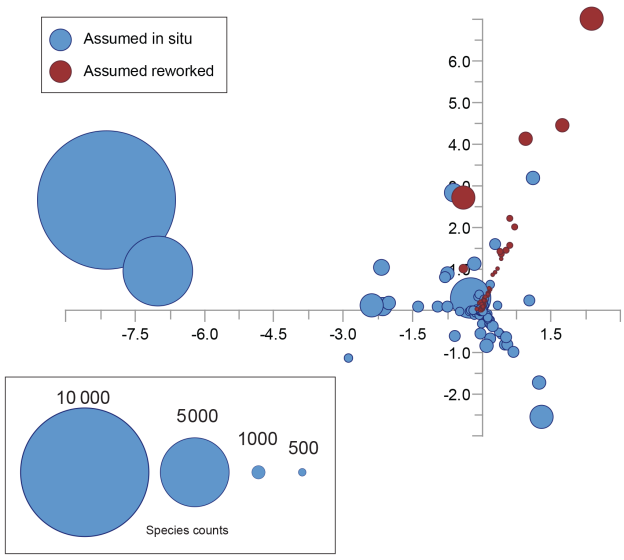

Figure 3. Principal component analysis plot showing species scores of the first two axes. Species that are a priori assumed to be reworked in are in red; species that are a priori assumed to be in situ are in blue (see Table 2 for species list, which species are assumed reworked, eigenvalues, axes scores and cumulative % of variance explained). Dot sizes indicate the total number of encounters in our analyses and gives an indication of the importance of that species in our data.

strata in our record are reworked uncertain. For instance, at IODP Site U1356 *Enneadocysta dictyostila* and *Deflandrea antarctica* are recorded throughout the lower Oligocene (Houben et al., 2013). Published stratigraphic last occurrences of these species in the Southern Ocean are ∼ 32 and ∼ 28 Ma, i.e. 1.5 and 4.5 Myr after the onset of the Oi-1 glaciation respectively (Brinkhuis et al., 2003a, b; Williams et al., 2004; Escutia et al., 2011). This suggests that both species may be deposited in situ in the lower Oligocene of IODP Hole 1356A. However, these last occurrences can be questioned given that rapid glaciation in the early Oligocene led in most places to a substantial sea-level drop (> 75 m equivalent sea level; see e.g. Houben et al., 2012, and references therein). This likely promoted reorganisation of continental shelves, erosion, and therewith a high likelihood of submarine reworking of Eocene shelf sediments into Oligocene deposits (see e.g. Pross et al., 2010). Indeed, these species are highly abundant in Eocene deposits throughout the Southern Ocean (Truswell, 1982; Warnaar et al., 2009; Bijl et al., 2011, 2013a, b), and today Eocene shelf deposits are exposed on the Wilkes Land margin (Escutia et al., 2011). To critically assess whether any dinocyst taxa recorded in the Oligocene–Miocene strata are reworked or in situ, we have performed a principal component analysis (PCA; ter Braak, 1986) on the quantitative dinocyst distribution data, using the C2 software program (Juggins, 2007), using square-root transformation. The reason why we hypothesise that we can

identify reworking with PCA is that we assume reworked species to have co-varying abundances in the record, which divert from the pelagic, in situ species variance. At the particular setting of IODP Site U1356 at the transition between the continental rise and the abyssal plain (Escutia et al., 2011), reworked species are brought to the site with bottom currents originating from the continental shelf. Higher continental shelf erosion would therefore increase the abundance of all reworked species relative to the abundance of in situ species. This would cause the reworked species to cluster together in PCAs. The variance distribution can therefore be used to verify our a priori assumptions of reworking.

4 Results

4.1 Identification of reworking based on principal component analysis

Of the 167 dinocyst species identified, 67 have positive scores on the first two PCA axes (Table 2; Fig. 3). Of these 67 species, we have a priori inferred 57 (85 %) of them to be reworked (Table 2 and Fig. 3). We do note that some of these species (e.g. *Spiniferites ramosus, Dapsilidinium pastielsii*) are actually extant species now found in lower-latitude environments (Zonneveld et al., 2013; Mertens et al., 2014). Given their relatively high abundance in Eocene sediments at the Wilkes Land margin (Bijl et al., 2013a), and their absence in these Southern Ocean high-latitude settings at present (Prebble et al., 2013; Zonneveld et al., 2013), we consider these species to be reworked from the Eocene. This also makes our inferences of labelling species in situ as conservative as possible. *Apectodinium* spp., *Charlesdowniea* spp., *Glaphyrocysta pastielsii* and *Membranophoridium perforatum* are stratigraphically confined to the early Eocene (Williams et al., 2004; Bijl et al., 2011, 2013a, b) and are hence obviously reworked. We observe a strict clustering of taxa that were a priori considered reworked, i.e. with positive scores on both axes, having low covariance with undoubtedly in situ taxa. This allows us to infer that the PCA covariance is to a substantial degree related to reworking of dinocysts. However, we infer 11 species with positive scores on the first two PCA axes (i.e. that cluster together with the reworked species) to be in situ: *Batiacasphaera compta*, *Cleistosphaeridium* sp. A, *Impagidinium elegans*, *I. patulum*, *I. paradoxum*, *Lejeunecysta adeliensis* sp. nov., *Palaeocystodinium golzowense*, *Reticulatosphaera actinocoronata*, *Stoveracysta kakanuiensis* and *Batiacasphaera* sp. D. Apart from *Cleistosphaeridium* sp. A and the newly described species *Lejeunecysta adeliensis*, these taxa have been repeatedly encountered in sediments straddling the Eocene–Oligocene boundary sediments (e.g. Sluijs et al., 2003; Eldrett et al., 2004; Egger et al., 2016). We report these taxa in low abundance (Table 2) in our record, predominantly within the interval characterised by a high degree of reworking in the lowermost Oligocene.

Table 3. Informal diagnoses of new dinocyst species found and reference to corresponding images in the plates.

	Pigmentation	Shape	Outline (l/b)	Apical horn	Lateral horns	Antapical horns	Cingulum	Figure; Plate
Lejeunecysta acuminata	Dark brown	Deflandroid	0.8–1	Pointed	Small to absent	Separated, pointed	Well-expressed	3a; 1A–G
Lejeunecysta katatonos	Beige	Rhomboidal	0.8–1.2	Small solid tip	Small solid tips	Small solid tip, connected	Not expressed	3b; 2H–M
Lejeunecysta attenuata	Transparent to light brown	Deflandroid	0.25–0.4	Hollow, very pointed	Absent	Closely spaced together, connected	Well-expressed	3c; 1N–O, 2A–C
Lejeunecysta rotunda	Dark brown	Rounded	0.9–1.1	Rounded	Rounded	Rounded, connected	Not expressed	3d; 2D–J
Lejeunecysta adeliensis sp. nov.	Beige	Rhomboidal	0.8–1	Small solid tip	Small solid tips	Small solid tip,disconnected	Not expressed	3e; 2K–O, 3A
Lejeunecysta cowiei	Beige	Deflandoid	0.8–1.2	Relatively long, solid tip	Absent	Separated, slender, pointed	Very wide	3f; 3B–C

This may explain the co-variance with evidently reworked species, as the reworking is most severe in the lower part of the Oligocene. Of the 100 species that do not have positive scores on the first two PCA axes, we would a priori infer 10 (10 %) a priori to be reworked: *Alisocysta circumtabulata*, *Cordosphaeridium funiculatum*, *Dapsilidinium pastielsii*, *Deflandrea antarctica*, *Diphyes colligerum*, *Enneadocysta dictyostila*, *E. multicornuta, Histiocysta palla, Manumiella druggii, Odontochitina* spp. and *Spinidinium schellenbergii*. The ranges of *Manumiella druggii* and *Odontochitina* spp. are restricted to the Cretaceous or lowermost Paleocene (Williams et al., 2004) and therefore are beyond doubt reworked in these Oligocene strata. Whether *Deflandrea antarctica* and *E. dictyostila/multicornuta* are reworked remains questionable because many sites show these species range into the Oligocene. However, the dominance of particularly these two species in Eocene records from the Southern Ocean (Brinkhuis et al., 2003b; Bijl et al., 2010, 2013b) suggests that they are reworked in the entire Oligocene–Miocene sequence at Site U1356. Despite these remaining uncertainties, our statistical analysis provides reasonably solid confirmation of our a priori inferences of reworking in our record.

4.2 Dinocyst taxonomy: formal description of two new species

Numerous previously unknown dinocyst species were encountered (Tables 2, 3; Fig. 4). Here we formally describe the new species *Lejeunecysta adeliensis* sp. nov., which we compare with the other species of *Lejeunecysta* (Table 4, Fig. 5) that have recently been described from the CRP drill cores (Clowes et al., 2016) and were also recognised at Site U1356 (Escutia et al., 2011; see Fig. 5 in this paper). Here we also formally describe a stratigraphically important new species: *Selenopemphix brinkhuisii* sp nov., the first occurrence of which defines the base of one of the dinocyst zones proposed here. The range top of this species is close to the top of magnetochron C12n. We also provide key diagnostic features for 23 other taxa (Table 3); the formal description of these other species will be published at a later stage.

Systematic paleontology

Division **Dinoflagellata** Bütschli 1885 (Fensome et al., 1993)

Subdivision **Dinokaryota** Fensome et al., 1993

Class **Dinophyceae** Pascher 1914

Subclass **Peridiniphycidae** Fensome et al., 1993

Order **Peridiniales** Haeckel 1984

Suborder **Peridiniineae** (autonym)

Family **Protoperidiniaceae** ex Bujak and Davies 1983 in Fensome et al. 1998, nom. cons. prop.

Genus *Lejeunecysta* Arztner and Dörhöfer 1978

Species *Lejeunecysta adeliensis* sp. nov. (Plate 2)

Diagnosis. Psilate species of *Lejeunecysta* with two distinct, isolated, slender, distally tapering antapical horns. The cyst has an exaggerated pentagonal outline due to the strong widening towards the cingulum of both the epicyst and the hypocyst. The cingulum itself is only expressed at both lateral sides, while barely visible on the dorsal and ventral sides.

Holotype. Integrated Ocean Drilling Program Hole U1356A, Core 95R section 1W, interval 64–68 cm, Slide 2; England Finder Coordinates (EFC) Q34; Plate 2K.

Paratype. Integrated Ocean Drilling Program Hole U1356A, Core 95R, Section 2W, interval 24–28 cm, Slide 2; EFC H33; Plate 2L.

Stratum typicum. Lower Oligocene of IODP Hole U1356A, Wilkes Land margin, Antarctica.
Etymology. Named after the type locality of the species, close to the Adélie Coast.

Description. An acavate cyst with a strong pentagonal outline. Both the epicyst and the hypocyst widen strongly towards the cingulum. The phragm is thin (< 1 µm) and psilate. The apex has straight lateral sides extending to a solid apical horn tip. The antapex is characterised by two separate, relatively long, slender horns that distally taper into a pointed tip. The wall of these pointed tips is thicker, resulting in solid ends of the horns. The archeopyle involves an iso- to slightly lati-deltaform second intercalary plate (2a) that is often adnate. The tabulation is only indicated by the archeopyle. The cingulum is marked by a set of parallel flanges along the lateral sides of the cyst, yet is absent on the dorsal and ventral sides. The cyst widens strongly from the anterior and posterior ends towards the cingulum, almost to form lateral horns. The sulcus is indiscernible on the specimens observed.

Dimensions. Holotype: 120×114 µm ($w \times l$). Paratype: 140×157 µm ($w \times l$). Average dimensions ($n = 6$): 130 µm (SD 14 µm) $\times$ 129 µm (SD 17 µm) ($w \times l$).
Stratigraphic distribution. During the first 1.5 million years following the Rupelian Oi-1 isotope excursion.

Geographic distribution. To date, *Lejeunecysta adeliensis* sp. nov. has only been recognised in the type section.

Affinities. *Lejeunecysta adeliensis* sp. nov. is different from all other *Lejeunecysta* species found at Site U1356 (see, e.g. Fig. 5). It most closely resembles *L. katatonos*, but differs from that species by having antapical horns that are completely separated rather than closely connected as in *L. katatonos*. The antapical horns of *L. adeliensis* sp. nov. are similar to those of *L. pulchra*, but the taxa differ in

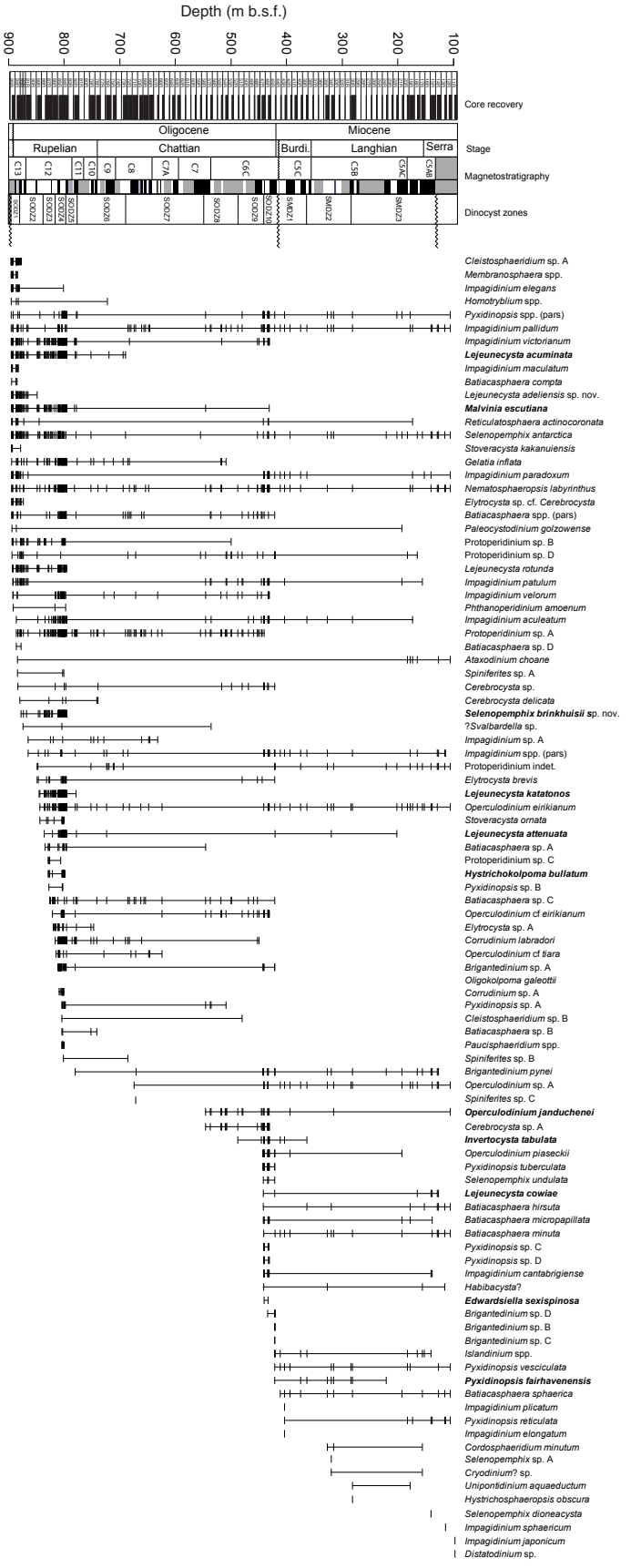

Figure 4. Stratigraphic chart of Oligocene–Miocene dinocyst species encountered at Site U1356, plotted in the order of first appearances. Age scale in Gradstein et al. (2012). Based on key events of species highlighted in boldface, a dinocyst zonation scheme is proposed (see Table 6 for definitions of zone boundaries).

Table 4. List of *Lejeunecysta* species encountered in Hole U1356A.

Species name	Plate	Brief informal description
Batiacasphaera sp. A		Species of *Batiacasphaera* that is relatively thin-walled and transparent. Specimens are also relatively large (> 80 µm)
Batiacasphaera sp. B		This is a species of *Batiacasphaera* with a reticulate autophragm that is reminiscent of that of *Cerebrocysta bartonensis*
Batiacasphaera sp. C	3J, K	A small species of *Batiacasphaera*, with a finely reticulate autophragm
Batiacasphaera sp. D		A small species of Batiacasphaera, inconspicuous, occurring only in the lower part of the Oligocene. Very rare.
Brigantedinium sp. A	4A–C	Species of *Brigantedinium* that has an endophragm that is similar to *Brigantedinium simplex* but with an irregular, finely fenestrate, thin, transparent autophragm
Brigantedinium sp. B		Large species of *Brigantedinium* with an autophragm bearing numerous densely spaced hair-like spines, giving it a "vilt-like" appearance
Brigantedinium sp. C		Species of *Brigantedinium* that does show some signs of paratabulation in the form of low septa
Brigantedinium sp. D		Species of *Brigantedinium* with a microreticulate autophragm
Cerebrocysta sp. A	4D	A large (> 80 µm) species of *Cerebrocysta*, with a relatively coarse reticulate autophragm
Cerebrocysta sp. B		Small (> 35 µm) cerebrocysta species with fine reticulate wall
Cleistosphaeridium sp. A		Small (about 40 µm) species of *Cleistosphaeridium*
Cleistosphaeridium sp. B		A large (> 80 µm) species of *Cleistosphaeridium*
Corrudinium sp. A	5A, B	A large (> 80 µm) species of *Corrudinium*, ornamentation similar to *Cerebrocysta* sp. A but with indications of paratabulation
Elytrocysta sp. A		Very large species of *Elytrocysta*, but bearing the characteristic closely appressed endo- and ectophragm
Operculodinium sp. A	7J, K	Species of *Operculodinium* with pronounced conical, pointed shape of the spines
Operculodinium cf. *eirikianum*		This species differs from *Operculodinium eirikianum* in being on average 3 times larger than the type species
Protoperidinium sp. A	8L–N	Species tentatively within the subfamily Congruentidioideae with dark pigmentation and numerous non-tabular spines. No apical, antapical or lateral horns visible
Protoperidinium sp. B		As Protoperidinium sp. A but lacking processes
Protoperidinium sp. C		Large cyst lacking apical, antapical or lateral horns and having a thin autophragm, giving it a transparent appeal
Protoperidinium sp. D	8K	As Protoperidinium sp. B but with paratabulation
Pyxidinopsis sp. A	8O	Small species with coarse reticulum
Pyxidinopsis sp. B	9H–K	Species of *Pyxidinopsis* with a "woolly" appearance of the wall
Pyxidinopsis sp. C		Species of medial size (∼ 40 µm) with coarse microfossulate autophragm.
Pyxidinopsis sp. D		Species of medial size (∼ 40 µm) with coarse microreticulum with high muri. Its ornamentation resembles that of the Eocene species *Pyxidinopsis waipawaensis*, but its overall size is smaller and its autophragm thinner
Selenopemphix sp. A		Species of *Selenopemphix* with microreticulate ornamentation
Spiniferites sp. A		Sensu Brinkhuis et al. 2003. *Spiniferites* with convex septa connecting the gonal processes, occasionally bearing sutural processes
Spiniferites sp. B		Species of *Spiniferites* that resembles the gonal protrusions of *Impagidinium aculeatum*
Spiniferites sp. C		Species within the *Spiniferites* complex, thick gonal processes like *Achomosphaera alcicornu*, but with sutural septa. Some specimens bear traberculae connecting some processes, resembling those of *Cannosphaeropsis*

(i) their overall outline, which is rounded in *L. pulchra* and more angular in *L. adeliensis* sp. nov., and (ii) the presence of parallel folds marking the cingulum on the lateral ends, which is typical for *L. adeliensis* sp. nov., but does not occur in *L. pulchra*.

Genus *Selenopemphix* Benedek 1972 emend. Bujak et al., 1980

Species *Selenopemphix brinkhuisii* sp. nov. (Plate 3)

Diagnosis. Species of *Selenopemphix* featuring crests on the longitudinal cingular sutures. On these septa as well as on some other sutures, numerous short, slender, conical spines arise, with pointed tips.

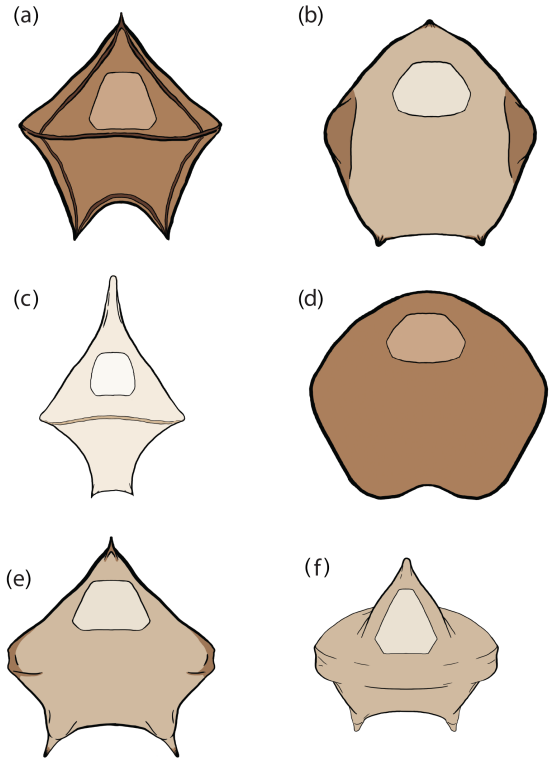

Figure 5. Schematic drawings of the six stratigraphically important species of *Lejeunecysta* found in the Site U1356 record (see Table 4 for the key morphologic characteristics). **(a)** *Lejeunecysta acuminata*; **(b)** *Lejeunecysta katatonos*; **(c)** *Lejeunecysta attenuata*; **(d)** *Lejeunecysta rotunda*; **(e)** *Lejeunecysta adeliensis* sp. nov.; **(f)** *Lejeunecysta cowiei*.

Holotype. Integrated Ocean Drilling Program Hole U1356A, Core 85R, Section 3W, interval 20–24 cm, Slide 1, EFC F32-4; Plate 3D.

Paratype. Integrated Ocean Drilling Program Hole U1356A Core 85R Section 3W, interval 100–104 cm, Slide 2, EFC L34-2; Plate 3E.

Stratum typicum. Lower Oligocene of IODP Hole U1356A, Wilkes Land margin, Antarctica.

Etymology. Named after Professor Henk Brinkhuis, in honour of his contributions to dinoflagellate cyst taxonomy, stratigraphy and paleoecology.

Description. Protoperidinioid cyst much wider than high. The autophragm is smooth, featuring short (2–5 µm), sharp, conical spines that are aligned on crests that follow sutures. The apical horn and the two antapical horns are blunt. The archeopyle involves the second intercalary plate (2a), which is somewhat rounded and often remains adnate. The tabulation is typical protoperidinioid whenever discernable. The sutures between the precingular and cingular plates as well as those between the cingulum and the postcingular plates bear short (2–4 µm) crests along which the spines are aligned. These septa seem interrupted at least, but not exclusively at the cingular plate boundaries. The sulcus is indented, giving the cyst outline in polar view the shape of a bent ellipse.

Dimensions. Holotype: 57×49 µm ($l \times d$). Paratype: 54×46 µm ($l \times d$). Average dimensions ($n = 9$): 59.4 µm (SD 5.3 µm) × 55.5 (SD 6.9 µm).

Stratigraphic distribution. In the type section, *Selenopemphix brinkhuisii* occurs between mid-C13n and mid-C12n. This equates to between 33.4 and 30.8 Ma.

Geographic distribution. To date, *Selenopemphix brinkhuisii* sp. nov. has only been recognised in the type section.

Affinities. *Selenopemphix brinkhuisii* sp. nov. differs from other spinose Selenopemphix species such as *S. brevispinosa*, *S. coronata*, *S. crenata, S. dioneacysta, S. islandensis, S. selenoides*, *S. warriensis* and *S. undulata* in also having spines on crests representing postcingular and precingular sutures. Furthermore, crests of *S. brinkhuisii* are discontinuous and not continuous such as in *S. undulata* and *S. selenoides*.

5 Discussion

5.1 Improved bio-magnetostratigraphic age model

Our high-resolution dinocyst biostratigraphy (Fig. 4) generally confirms the published age model for the Oligocene and Miocene interval of Hole U1356A (Tauxe et al., 2012); we have refined the age control around the Oligocene–Miocene boundary. New dinoflagellate cyst events recognised in this study enabled the identification of the position and constrained the duration of the hiatus around the Oligocene–Miocene boundary. Specifically, the presence of *Edwardsiella sexispinosa* in samples from Cores 47R and 46R (Fig. 4) confirms that these cores are close to the Oligocene–Miocene boundary: at nearby Ocean Drilling Program (ODP) Site 1168, the first stratigraphic occurrence (FO) of *E. sexispinosa* is around 22.5 Ma (Brinkhuis et al., 2003a). The FO of *E. sexispinosa* was detected in sediments that still contain late Oligocene calcareous microfossils (Tauxe et al., 2012): the last stratigraphic occurrence (LO) of *Reticulofenestra bisecta* in Core 46R (22.97 Ma) and *Globigerina euapertura* (23.0 Ma) in Core 45R suggest that *E. sexispinosa* has an older FO on the Antarctic margin than in southern Australia. In turn, we suggest that the reversed magnetic polarities in Cores 45–46R correlate to the youngest Oligocene reversed intervals: C6Cn.2r and C6Cn.1r (Brinkhuis et al., 2003a).

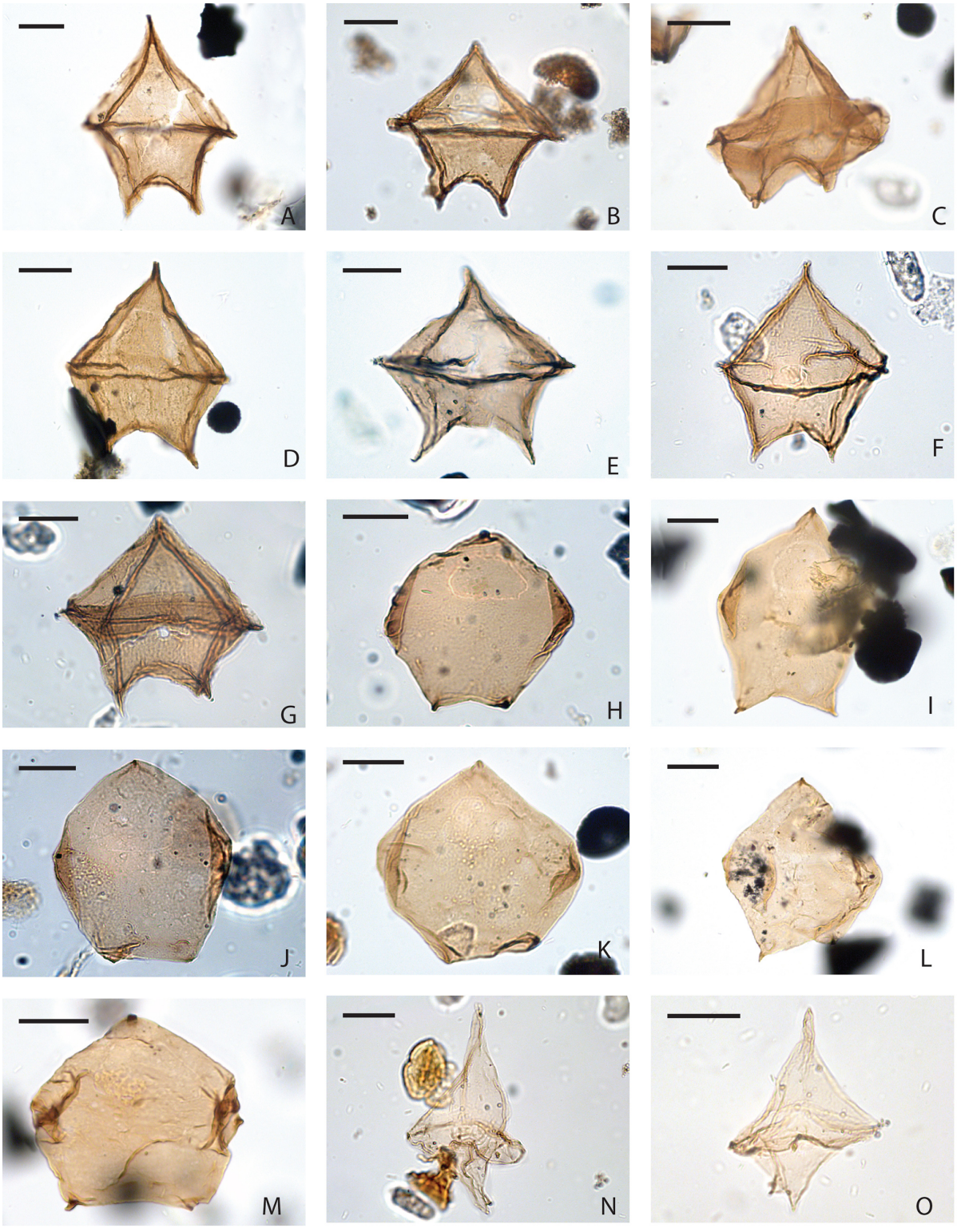

Plate 1. **(A–G)** *Lejeunecysta acuminata*. **(A)** Integrated Ocean Drilling Program (IODP) Hole U1356A, Core 85R, Section 5W, interval 80–84 cm; **(B)** 84R-1W, 61–64 cm; **(C)** 85R-4W, 100–104 cm; **(D)** 85R-5W, 100–104 cm; **(E)** 85R-5W, 100–104 cm; **(F)** 87R-3W, 40–44 cm; **(G)** 89R-2W, 39–43 cm. **(H–M)** *Lejeunecysta katatonos*. **(H)** 84R-4W, 120–124 cm; **(I)** 85R-5W, 100–104 cm; **(J)** 89R-2W, 39–43 cm; **(K)** 84R-5W, 0–4 cm; **(L)** 85R-5W, 100–104 cm; **(M)** 84R-6W, 0–4 cm. **(N–R)** *Lejeunecysta attenuata*. **(N)** 84R-4W, 39–43 cm; **(O)** 84R-4W, 39–43 cm; scale bar is 25 µm.

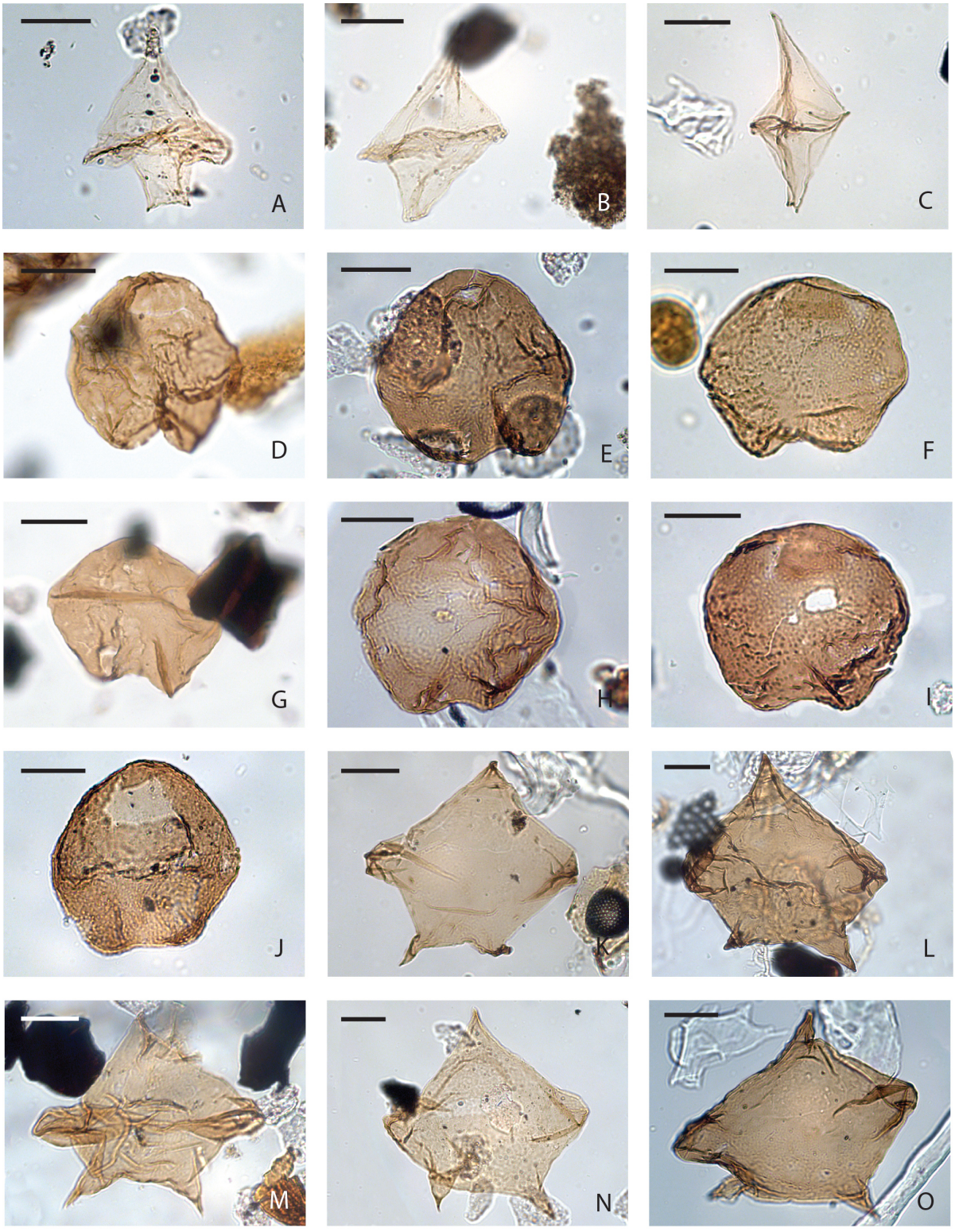

Plate 2. **(A–C)** *Lejeunecysta attenuata*. **(A)** Integrated Ocean Drilling Program Hole U1356A, Core 84R, Section 4W, interval 39–43 cm; **(B)** 84R-1W, 61–65 cm; **(C)** 94R-4W, 4–8 cm. **(D–J)** *Lejeunecysta rotunda*. **(D)** 85R-4W, 60–64 cm; **(E)** 93R-2W, 4–8 cm; **(F)** 93R-1W, 6–10 cm; **(G)** 85R-5W, 57–61 cm; **(H)** 94R-1W, 144–148 cm; **(I)** 93R-3W, 103–107 cm; **(J)** 91R-5W, 44–48 cm. **(K–O)** *Lejeunecysta adeliensis* sp. nov. **(H)** Holotype 95R-1W, 64–68 cm, Slide 2; England Finder Coordinates (EFC) Q34. **(I)** Paratype 95R-2W, 24–28 cm, Slide 2; EFC H33; **(J)** 93R-2W, 4–8 cm; **(K)** 93R-1W, 24–28 cm; **(L)** 94R-4W, 4–8 cm; scale bar is 25 µm.

Table 5. Dinocyst zone boundaries: depths and calibrated ages.

Zone	Bottom definition	Top definition	Bottom sample U1356A-	Top sample U1356A-	Bottom depth (m b.s.f.)	Top depth (m b.s.f.)	Bottom calibration	Top calibration	Bottom age (Ma)	Top age (Ma)
SMDZ3	FO *Unipontidinium aquaeductum*	Overlying zone	30R-4W, 20–22	14R-3W, 20–22	282.21	127.31	75 % in C5Bn.2n	33 % between FO *Actinomma golowini* and FO *Denticulopsis praedimorpha*	15.1	Undefined
SMDZ2	LO *Invertocysta tabulata*	Overlying zone	39R-1W, 20–22	30R-6W, 20–22	363.81	284.61	100 % in C5Cn.2n	75 % in C5Bn.2n	16.3	15.1
SMDZ1	FO *Pyxidinopsis fairhavenensis*	Overlying zone	44R-1W, 20–24	40R-2, 19–21	411.81	374.9	50 % in C6Cn.2n	100 % in C5Cn.2n	22.9	16.3
SODZ10	FO *Edwardsiella sexispinosa*	Overlying zone	47R-1W, 45–49	45R-1w, 10–14	440.87	421.31	50 % in C6Cn.2r	50 % in C6Cn.2n	23.1	22.9
SODZ9	FO *Invertocysta tabulata*	Overlying zone	52R-CCW, 9–13	47R-1W, 64–68	488.31	441.06	50 % in C6Cr	50 % in C6Cn.2r	23.6	23.1
SODZ8	FO *Operculodinium janduchenei*	Overlying zone	58R-1W, 19–21	53R-2W, 20–22	545.6	499.46	50 % in C7n	50 % in C6Cr	24.2	23.6
SODZ7	LO *Lejeunecysta acuminata*	Overlying zone	72R-5W, 18–20	59R-1W, 17–19	685.43	555.18	50 % in C8r	50 % in C7n	26.2	24.2
SODZ6	LO *Lejeunecysta katatonos*	Overlying zone	82R-2W, 40–44	73R-1W, 18–20	777.62	689.59	Base C11n.1n	50 % in C8r	29.5	26.2
SODZ5	LO *Hystrichokolpoma bullatum*	Overlying zone	84R-3W, 0–4	82R-3W, 40–44	798.02	778.96	50 % between top C12n and base C11n.1n	Base C11n.1n	30.0	29.5
SODZ4	FO *Corrudinium labradori*	Overlying zone	86R-2W, 40–44	84R-3W, 19–23	816.2	798.21	Top C12n	50 % between top C12n and base C11n.1n	31.0	30.0
SODZ3	FO *Lejeunecysta attenuata*	Overlying zone	88R-2W, 98–102	86R-3W, 40–44	835.86	817.41	50 % in C12R	Top C12n	32.1	31.0
SODZ2	FO *Selenopemphix brinkhuisii* sp. nov.	Overlying zone	93R-2W, 44–48	89R-1W, 44–48	878.41	843.56	95 % in C13n	50 % in C12r	33.2	32.1
SODZ1	FO *M. escutiana*	Overlying zone	95R-3W, 82–85	93R-3W, 44–48	894.7	879.51	Mid-Oi-1 isotope shift	95 % in C13n	33.7	33.2

The normal polarity at the top of Core 46R (Fig. 4) then correlates to C6Cn.3n. We then extrapolate this to Core 45R, which has normal magnetic polarity and, based on the absence of typical Miocene marker species, should correlate to C6Cn.2n: the Oligocene–Miocene boundary. Our interpretation slightly differs from the interpretation published in Tauxe et al. (2012), which infers the onset of C6Cn.2n in Core 46R and the hiatus to be somewhere between 432 and 402 m b.s.f. (Cores 45R–43R; Tauxe et al., 2012). Our correlation of high-resolution dinocyst biostratigraphy and the available paleomagnetic signal indicates that the hiatus lies between Cores 44R and 45R, and Core 45R falls within the Mi-1 glaciation (Fig. 2).

5.2 Provisional dinocyst zonation scheme

We have identified 13 key (regional) dinocyst extinction or origination events (bold in Figs. 4, 6) from all the in situ dinocysts (Fig. 4). We prioritised those dinocyst events that had relatively high abundances, had sharp appearances or extinctions and can be calibrated well to magneto-subchrons. These index events form the basis for the Oligocene–Miocene Southern Ocean dinocyst zonation proposed here (see Table 5 for an overview of zone boundary definitions), which comprises 10 zones for the Oligocene and 3 zones for the Miocene. We name the zones as Southern Ocean Oligocene Dinocyst Zone (SODZ) or Southern Ocean Miocene Dinocyst Zone (SMDZ). We acknowledge that the zonation is incomplete due to a hiatus covering the early Miocene (22.5–17 Ma) and one encompassing the mid-Miocene (13–10.8 Ma) and the occasional low core recovery. We calibrate the ages of the zone boundaries to the GPTS by indicating foremost where in existing magnetostratigraphic chrons the zone boundaries occur. This is consistently indicated as a percentage into a certain chron, measured from the bottom, and by assuming linear sedimentation rates between reversals in our record.

5.2.1 Zone SODZ1

Base definition. The base of this zone is defined by the FO of *Malvinia escutiana*.

Top definition. The top of this zone is defined by the base of SODZ2, i.e. the FO of *Selenopemphix brinkhuisi*, sp. nov.

Type locality. IODP Site U1356.

Base sample. U1356A-95R-3W, 82–85 cm (894.7 m b.s.f.).

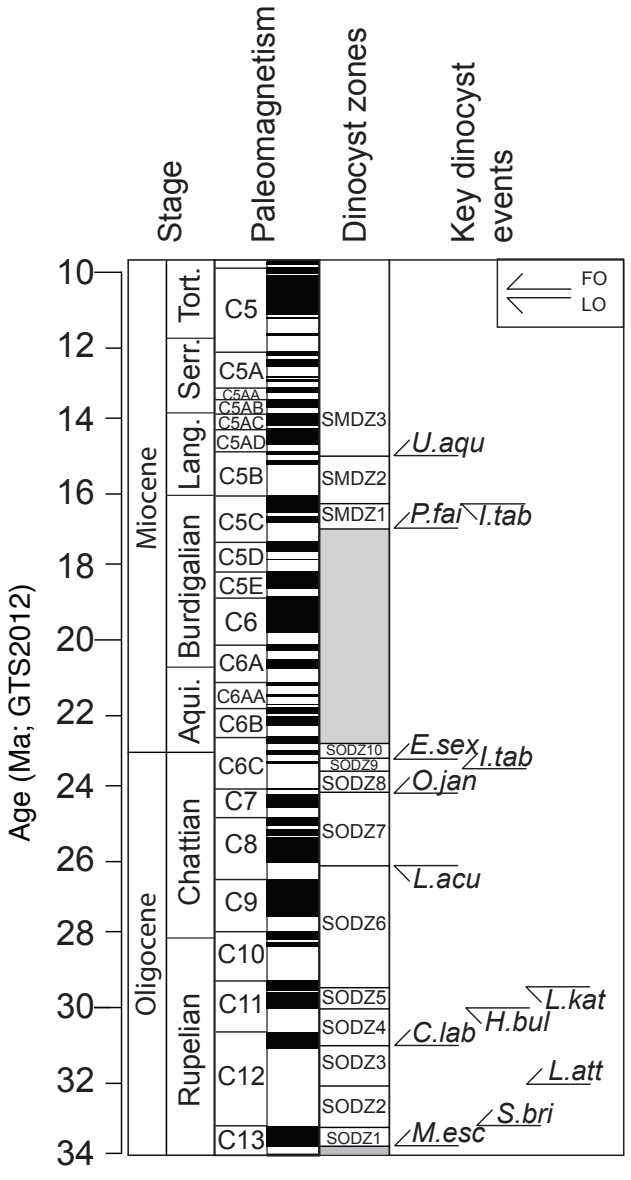

Figure 6. Summary of the dinocyst zones proposed in this paper for the Oligocene–Miocene Southern Ocean. See Table 5 for a summary of the depth and age data. M.esc: *Malvinia escutiana*; S.bri: *Selenopemphix brinkhuisii*; L.att: *Lejeunecysta attenuata*; C.lab: *Corrudinium labradori*; H.bul: *Hystrichokolpoma bullatum*; L.kat: *Lejeunecysta katatonos*; L.acu: *Lejeunecysta acuminata*; O.jan: *Operculodinium janduchenei*; I.tab: *Invertocysta tabulata*; E.sex: *Edwardsiella sexispinosa*; P.fai: *Pyxidinopsis fairhavenensis*; U.aqu: *Unipontidinium aquaeductum*.

Top sample. U1356A-93R-3W, 44–48 cm (879.51 m b.s.f.).

Calibration. The base of this zone might be included in a 14 Myr hiatus at the type locality. At DSDP Site 511, the FO of *Malvinia escutiana* is correlative with the Oi-1 isotope excursion (Houben et al., 2011), thus occurring in the earliest Oligocene (e.g. Coxall and Wilson, 2011). On the basis of this calibration, we calibrate the base of Zone SODZ1 to the Oi-1 isotope excursion. The top of the zone is calibrated to ~95 % in C13n.

Age. 33.7–33.2 Ma.

Characteristic species. At the type locality, this dinocyst zone is dominated by the abundance of what we infer are reworked late Eocene dinocysts; species that are considered in situ include *Malvinia escutiana, Lejeunecysta fallax, L. acuminata*, *L. rotunda,* abundant *Selenopemphix nephroides* and *S. antarctica, Reticulatosphaera actinocoronata*, *Impagidinium* cf. *aculeatum, I. velorum,* and *I. paradoxum.*

Significant events. Several *Impagidinium* species have (regional) first occurrences in this zone, such as *I. patulum* and *I.* cf. *aculeatum*. *Phthanoperidinium amoenum* has an FO in this zone.

Remarks. This dinocyst zone covers the onset and first 1 million years of glaciation of Antarctica. The abundance of reworked (middle to late) Eocene dinocysts in the Oligocene sequence suggests that the time interval represented in this dinocyst zone is characterised by a relatively rapid (~200 kyr) glacial advance followed by a gradual retreat of the ice sheet.

5.2.2 Zone SODZ2

Base definition. The base of this zone is defined by the first stratigraphic occurrence of *Selenopemphix brinkhuisii* sp. nov.

Top definition. The top of this zone is defined by the base of SODZ3, i.e. the FO of *Lejeunecysta attenuata*.

Type locality. IODP Site U1356.

Base sample. U1356A-93R-2W, 44–48 cm (878.41 m b.s.f.).

Top sample. U1356A-89R-1W, 44–48 cm (843.56 m b.s.f.).

Calibration. The base of this zone is calibrated to 95 % in C13n; the top is calibrated to the 50 % in C12r.

Age. 33.2–32.1 Ma.

Characteristic species. This interval is characterised by a dominance of *Lejeunecysta* spp. and *Brigantedinium* spp., while *Selenopemphix* spp. and *Malvinia escutiana* decline in abundance.

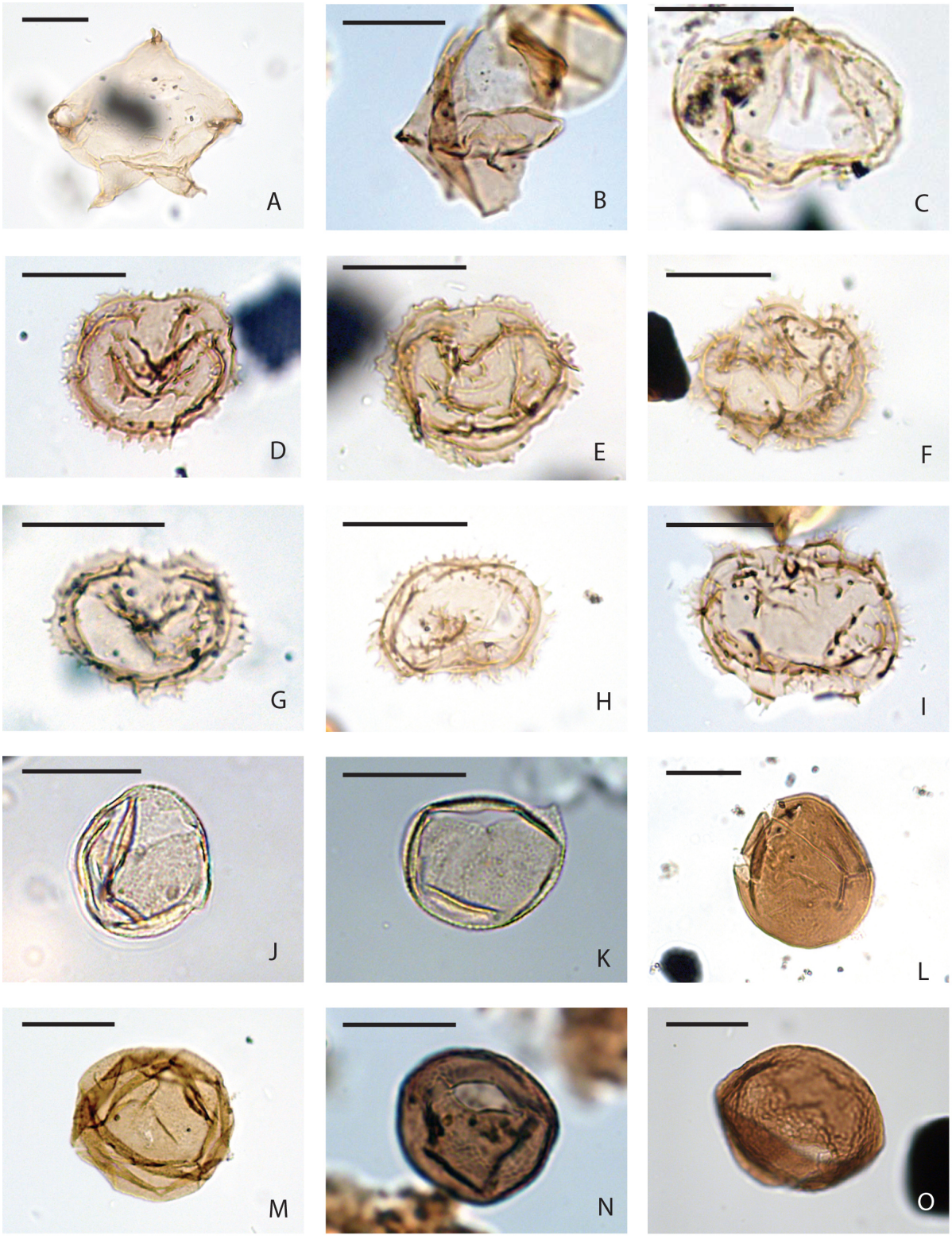

Plate 3. *Lejeunecysta adeliensis* sp. nov. **(A)** Integrated Ocean Drilling Program Hole U1356A, Core 85R, Section 5W, interval 80–84 cm. **(B, C)** *Lejeunecysta cowiei*. **(B)** 17R-1W, 20–22 cm. **(C)** 14R-3W, 20–22 cm. **(D–I)** *Selenopemphix brinkhuisii* sp. nov. **(D)** Holotype 85R-3W, interval 20–24 cm Slide 1 England Finder Coordinates (EFC) F32-4. **(E)** Paratype 85R-3W, 100–104 cm slide 2 EFC L34-2; **(F)** 85R-4W, 100–104 cm; **(G)** 85R-4W, 100–104 cm; **(H)** 85R-4W, 60–64 cm; **(I)** 85R-4W, 100–104 cm; **(J)** *Batiacasphaera* sp. C 44R-1W, 20–24 cm; **(K)** *Batiacasphaera* sp. C 34R-1W, 27–29 cm; **(L, M)** *Brigantedinium simplex* **(L)** 92R-3W, 44–48 cm; **(M)** 85R-4W, 60–64 cm; **(N, O)** *Brigantedinium pynei* **(N)** 17R-1W, 20–22 cm; **(O)** 21R-2W, 20–22 cm; scale bar is 25 µm.

Significant events. This zone includes the FO of *Operculodinium eirikianum*.

Remarks. This zone correlates to a time interval of further warming and Antarctic ice retreat, as interpreted from the benthic foraminiferal oxygen isotope compilation of Pälike et al. (2006). Of particular interest is the near disappearance *Selenopemphix antarctica* because today high abundances of this species are strongly tied to the sea-ice ecosystem of coastal Antarctica (Prebble et al., 2013).

5.2.3 Zone SODZ3

Base definition. The base of this zone is defined by the first stratigraphic occurrence of *Lejeunecysta attenuata*.

Top definition. The top of this zone is defined by the base of SODZ4, i.e. the FO of *Corrudinium labradori*.

Type locality. IODP Site U1356.

Base sample. U1356A, 88R-2W, 98–102 cm (835.86 m b.s.f.).

Top sample. U1356A, 86R-3W, 40–44 cm (817.41 m b.s.f.).

Calibration. The base is calibrated to 50 % in C12r; the top of the zone is calibrated to the C12r–C12n boundary.

Age. 32.1–31.0 Ma.

Characteristic species. This zone is characterised by the abundance of *Lejeunecysta* spp. Furthermore, *Selenopemphix brinkhuisii* sp. nov. is common in this interval.

Significant events. This zone sees the FO of several new *Batiacasphaera* and Protoperidinioid species, *Hystrichokolpoma bullatum,* and *Operculodinium* sp. cf. *eirikianum.*

5.2.4 Zone SODZ4

Base definition. The base of this zone is defined by the FO of *Corrudinium labradori.*

Top definition. The top of this zone is defined by the base of SODZ5, i.e. the LO of *Hystrichokolpoma bullatum*.

Type locality. IODP Site U1356.

Base sample. U1356A, 86R-2W, 40–44 cm (816.20 m b.s.f.).

Top sample. U1356A, 84R-3W, 19–23 cm (798.21 m b.s.f.).

Calibration. The base of the zone is calibrated to the C12n–C12r boundary, while the top is calibrated to 50 % between the top of C12n and the base of C11n.1n.

Age. 31.0–30.0 Ma.

Characteristic species. The top of the zone sees a rapid increase in various morphotypes of protoperidioid dinocysts that cannot be placed within *Brigantedinium* spp., *Lejeunecysta* spp. or *Selenopemphix* spp. Almost throughout the zone, many specimens of *Brigantedinium* spp. have a discontinuous, transparent, perforated second outer wall layer (Plate 3G–I).

Significant events. This zone includes the range of *Oligokolpoma galeottii*, the LO of *Phthanoperidinium amoenum*, *Protoperidinium* sp. C, and *Corrudinium* sp. A, and the FO of *Corrudinium* sp. A, *C. devernaliae* and cavate *Brigantedinium.*

5.2.5 Zone SODZ5

Base definition. The base of this zone is defined by the LO of *Hystrichokolpoma bullatum.*

Top definition. The top of this zone is defined by the base of SODZ6, i.e. the LO of *Lejeunecysta katatonos*.

Type locality. IODP Site U1356.

Base sample. U1356A, 84R-3W, 0–4 cm (798.02 m b.s.f.).

Top sample. U1356A, 82R-3W, 40–44 cm (778.96 m b.s.f.).

Calibration. The base of this zone is calibrated to 50 % between the top of C12n and the base of C11n.1n, the top to the base of C11n.1n.

Age. 30.0–29.5 Ma.

Characteristic species. This zone sees the first pulse of dominance of new *Protoperidinium* taxa that cannot be placed in the more common existing genera *Lejeunecysta, Selenopemphix* spp. and *Brigantedinium* spp.

Significant events. The (regional) LO of *Tectatodinium pellitum*, *Lejeunecysta rotunda, L. katatonos,* cavate *Brigantedinium,* and *Selenopemphix brinkhuisii* sp. nov., and the FO of *B. pynei*, occur in this zone.

Remarks. *Tectatodinium pellitum* is considered a thermophilous species in the North Sea area in the Pliocene (Head, 1994).

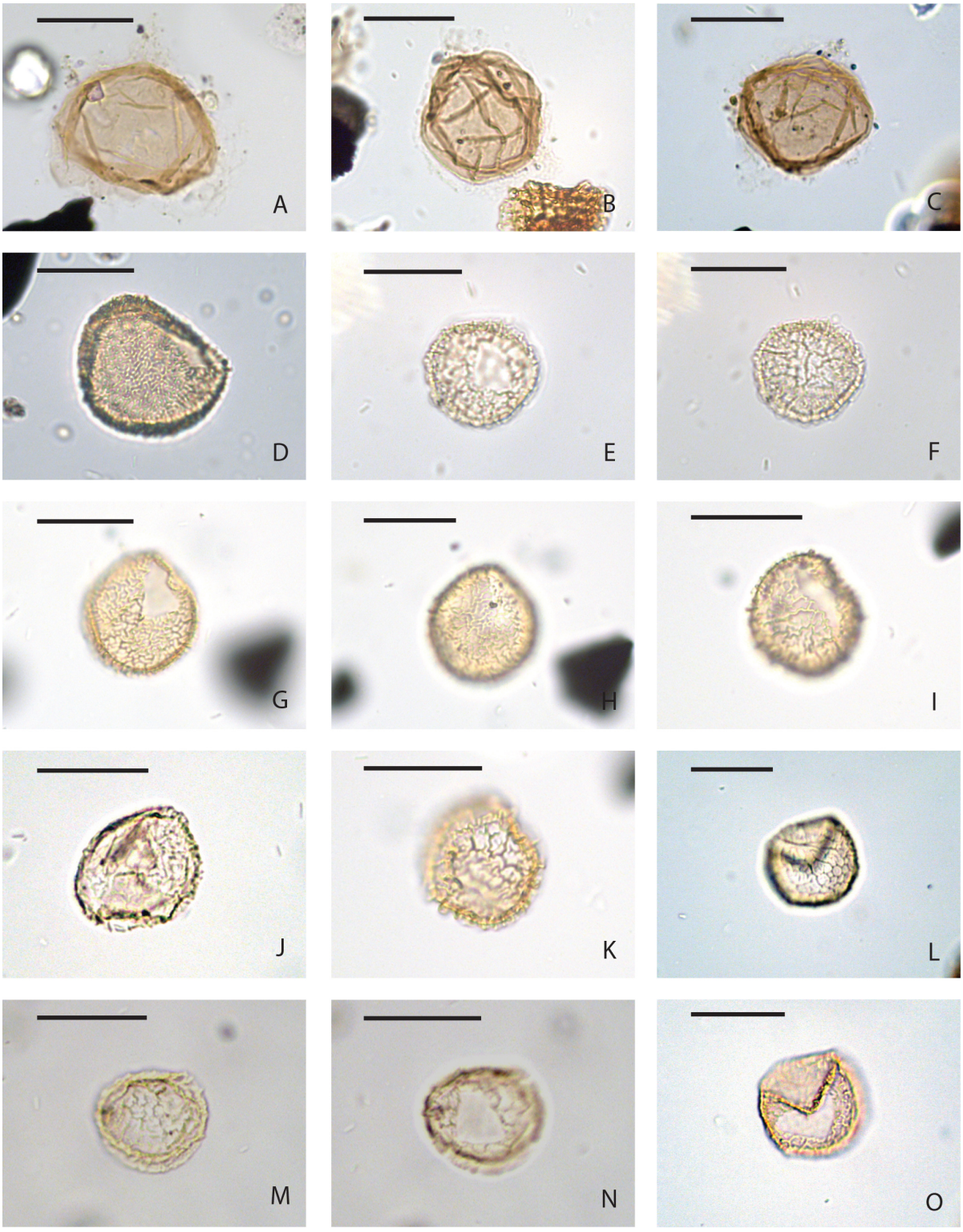

Plate 4. **(A–C)** *Brigantedinium* sp. A. **(A)** Integrated Ocean Drilling Program Hole U1356A, Core 85R, section 4W, interval 60–64 cm; **(B)** 84R-4W, 120–124 cm; **(C)** 85R-2W, 96–100 cm; **(D)** *Cerebrocysta* sp. A 84R-4W, 39–43 cm; **(E–O)** *Corrudinium labradori* **(E, F)** 84R-5W, 0–4 cm; **(G, H)** 84R-6W, 0–4 cm; **(I)** 84R-7W, 60–64 cm; **(J)** 85R-5W, 39–43 cm; **(K)** 84R-7W, 60–64 cm; **(L, M)** 85R-4W, 100–104 cm; **(N, O)** 85R-5W, 100–104 cm. Scale bar is 25 µm.

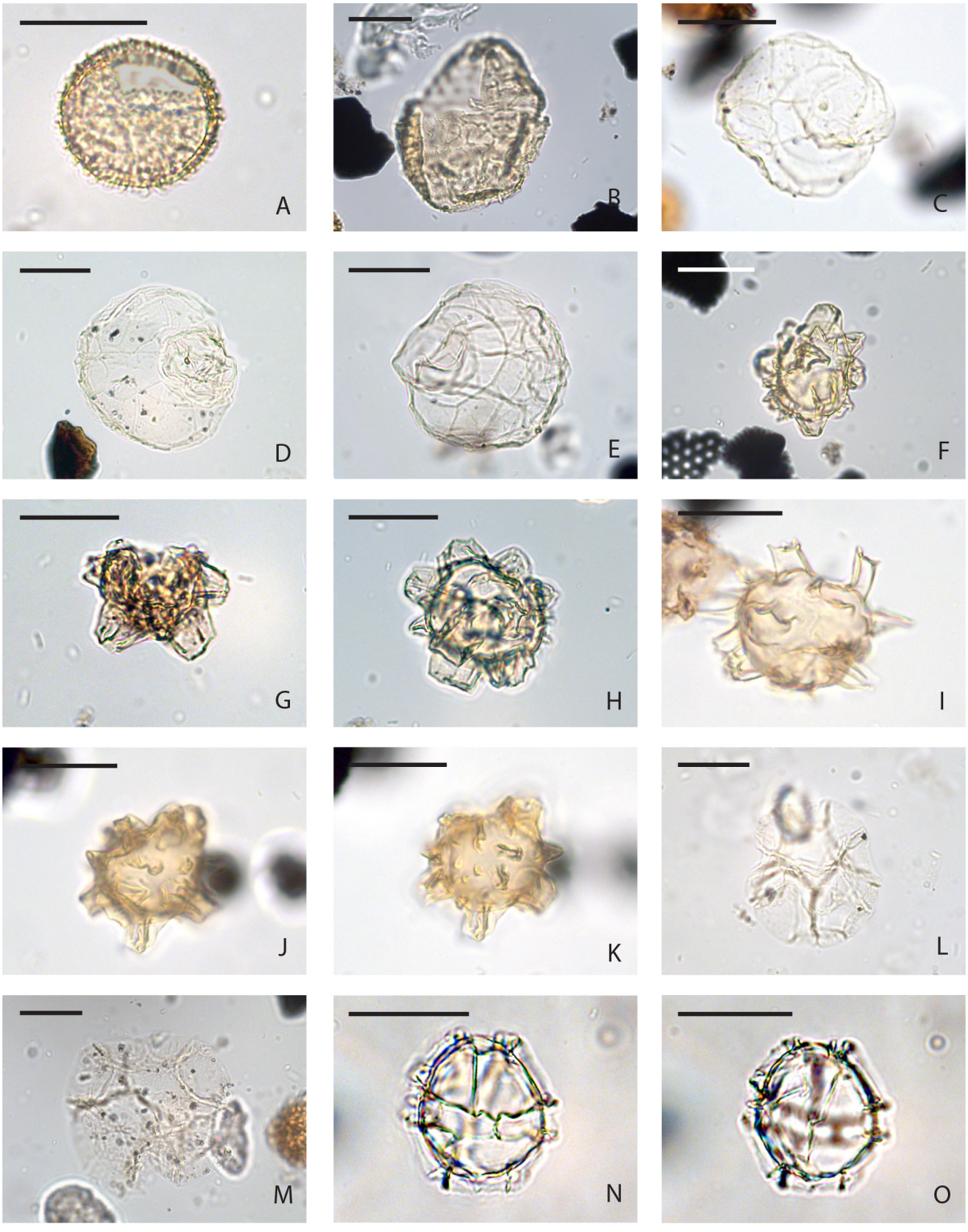

Plate 5. **(A, B)** *Corrudinium* sp. **(A)** Integrated Ocean Drilling Program Hole U1356A, Core 84R, Section 4W, interval 39–43 cm; **(B)** 84R-4W, 120–124 cm; **(C–E)** *Gelatia inflata* **(C)** 85R-5W, 80–84 cm; **(D)** 91R-4W, 104–108 cm; **(E)** 84R-4W, 120–124 cm; **(F–H)** *Hystrichokolpoma bullatum* F 84R-4W, 80–84 cm; G 84R-5W, 0–4 cm; **(H)** 84R-5W, 0–4 cm; **(I, J)** *Hystrichokolpoma truncatum* **(I)** 84R-6W, 0–4 cm **(J, K)** 84R-7W, 60–64 cm; **(L, M)** *Impagidinium pallidum* **(L)** 47R-4W, 85–89 cm; **(M)** 52R-CCW, 9–13 cm; **(N, O)** *Impagidinium* sp. 44R-1W, 20–24 cm; scale bar is 25 µm.

5.2.6 Zone SODZ6

Base definition. The base of this zone is defined by the LO of *Lejeunecysta katatonos.*

Top definition. The top of this zone is defined by the base of SODZ7, i.e. the LO of *Lejeunecysta acuminata*.

Type locality. IODP Site U1356.

Base sample. U1356A, 82R-2W, 40–44 cm (777.62 m b.s.f.).

Top sample. U1356A, 73R-1W, 18–20 cm (689.59 m b.s.f.).

Calibration. The base of this zone is calibrated to the base of C11n.1n, while the top of this zone is here calibrated to 50 % in C8r.

Age. 29.5–26.2 Ma.

Characteristic species. This zone is characterised by low-diversity assemblages. Protoperidinioid dinocysts of different and in some cases unclear genera are dominant.

Significant events. The LO of *Malvinia escutiana* occurs at the top of the zone.

5.2.7 Zone SODZ7

Base definition. The base of this zone is defined by the LO of *Lejeunecysta acuminata.*

Top definition. The top of this zone is defined by the base of SODZ8, i.e. the FO of *Operculodinium janduchenei*.

Type locality. IODP Site U1356.

Base sample. U1356A, 72R-5W, 18–20 cm (685.43 m b.s.f.).

Top sample. U1356A, 59R-1W, 17–19 cm (555.18 m b.s.f.).

Calibration. The base is calibrated to 50 % in C8r, while the top is calibrated to 50 % in C7n.

Age. 26.2–24.2 Ma.

Characteristic species. There is a high abundance of *Brigantedinium* spp., and the diversity of this zone is relatively low.

Significant events. The lower half of this zone is characterised by the occasional high abundance of a variety of chorate and proximate acritarchs. The zone contains the FO of *Operculodinium* sp. C.

5.2.8 Zone SODZ8

Base definition. The base of this zone is defined by the FO of *Operculodinium janduchenei*.

Top definition. The top of this zone is defined by the base of SODZ9, i.e. the FO of *Invertocysta tabulata*.

Type locality. IODP Site U1356.

Base sample. U1356A, 58R-1W, 19–21 cm (545.60 m b.s.f.).

Top sample. U1356A, 53R-2W, 20–22 cm (499.46 m b.s.f.).

Calibration. The base of this zone is calibrated to 50 % in C7n, while the top of this zone is calibrated to 50 % in C6Cr.

Age. 24.2–23.6 Ma.
Characteristic species. This zone is characterised by the abundance of gonyaulacoid dinocyst genera such as *Impagidinium* spp., *Operculodinium* spp., *Batiacasphaera* spp. and *Spiniferites* spp. at the expense of the abundance of protoperidinioid dinocysts.

Significant events. The LOs of *Batiacasphaera* sp. A, *Corrudinium devernaliae* and *Gelatia inflata* are within this zone. The FOs of *Operculodinium janduchenei* and *Cerebrocysta* sp. A are also within this zone. There is also a conspicuously high presence of small chorate acritarchs.

5.2.9 Zone SODZ9

Base definition. The base of this zone is defined by the FO of *Invertocysta tabulata*.

Top definition. The top of this zone is defined by the base of SMDZ1, i.e. the FO of *Edwardsiella sexispinosa*.

Type locality. IODP Site U1356.

Base sample. U1356A, 52R-CCW, 9–13 cm (488.31 m b.s.f.).

Top sample. U1356A, 47R-1W, 64–68 cm (441.06 m b.s.f.).

Calibration. The base of this zone is calibrated to 50 % in C6Cr, while the top is calibrated to 80 % in C6Cn.2r

Age. 23.6–23.0 Ma.

Characteristic species. The most abundant genera are *Brigantedinium* spp. and indeterminable Protoperidinioid cysts, while gonyaulacoid cysts are also present to common.

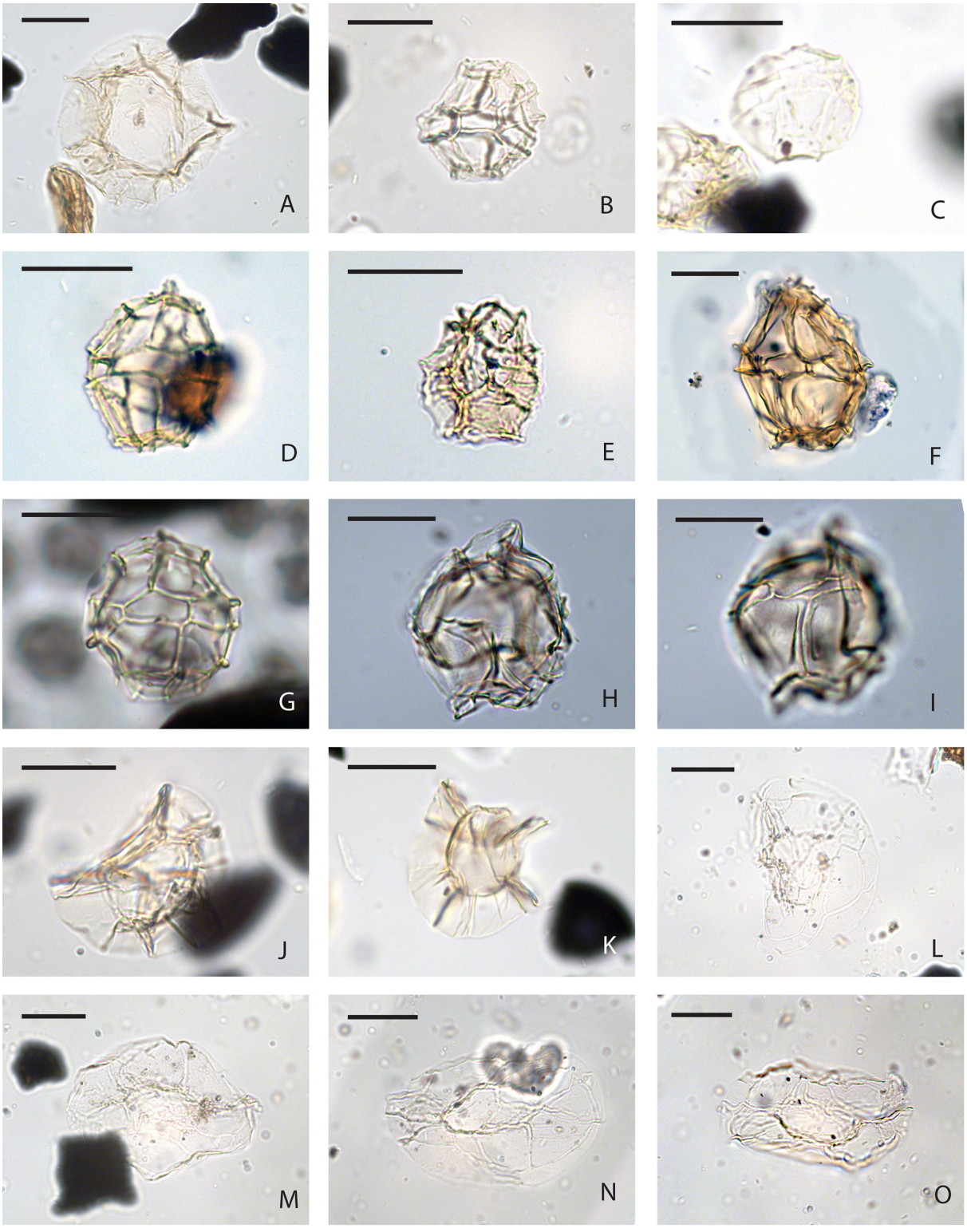

Plate 6. **(A)** *Impagidinium pallidum* Integrated Ocean Drilling Program Hole U1356A, Core 85R-, Section 1W, interval 20–24 cm; **(B)** *Impagidinium* sp. 47R-1W, 26–30 cm; **(C)** *Impagidinium* sp. 85R-5W, 57–61 cm; **(D)** *Impagidinium* sp. 85R-5W, 100–104 cm; **(E)** *Impagidinium* sp. 91R-4W, 104–108 cm; **(F)** *Impagidinium* sp. 85R-5W, 57–61 cm. **(G)** 39R-1W, 20–22 cm; **(H, I)** *Impagidinium* sp. 40R-2W, 19–21 cm; **(J, K)** *Impagidinium velorum* 84R-4W, 120–124 cm; **(K)** 84R-7W, 60–64 cm; **(L–O)** *Invertocysta tabulata* 52R-CCW, 9–13 cm; **(M)** 52R-CCW, 9–13 cm; **(N)** 52R-CCW, 9–13 cm; **(O)** 52R-CCW, 9–13 cm. Scale bar is 25 µm.

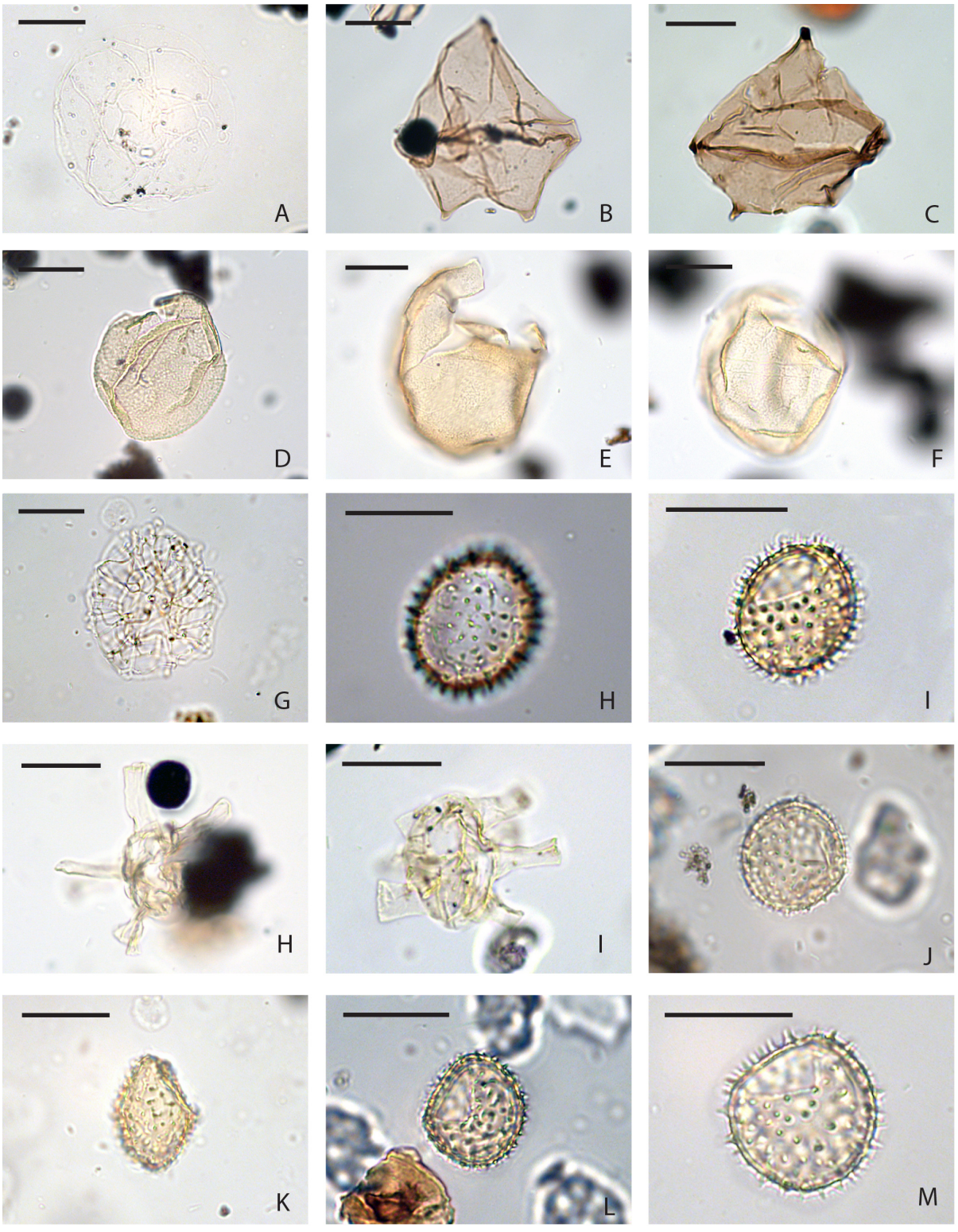

Plate 7. **(A)** *Invertocysta tabulata*, Integrated Ocean Drilling Program Hole U1356A, Core 44R, Section 1W, interval 20–24 cm; **(B, C)** *Lejeunecysta fallax* **(B)** 17R-1W, 20–22 cm; **(C)** 17R-3W, 20–22 cm; **(D–F)** *Malvinia escutiana* **(D)** 84R-5W, 120–124 cm; **(E)** 84R-6W, 0–4 cm; **(F)** 84R-6W, 0–4 cm; **(G)** *Nematosphaeropsis labyrinthus* 47R-4W, 85–89 cm; **(H, I)** *Oligokolpoma galeottii* **(H)** 85R-5W, 39–43 cm; **(I)** 85R-5W, 57–61 cm. **(J, K)** *Operculodinium* sp. A 44R-1W, 20–24 cm; **(L, M)** *Operculodinium janduchenei* **(L)** 46R-1W, 68–72 cm; **(M)** 47R-1W, 26–30 cm; **(N)** *Operculodinium* cf. *janduchenei* 46R-1W, 68–72 cm; **(O)** *Operculodinium piaseckii* 44R-1W, 20–24 cm; scale bar is 25 µm.

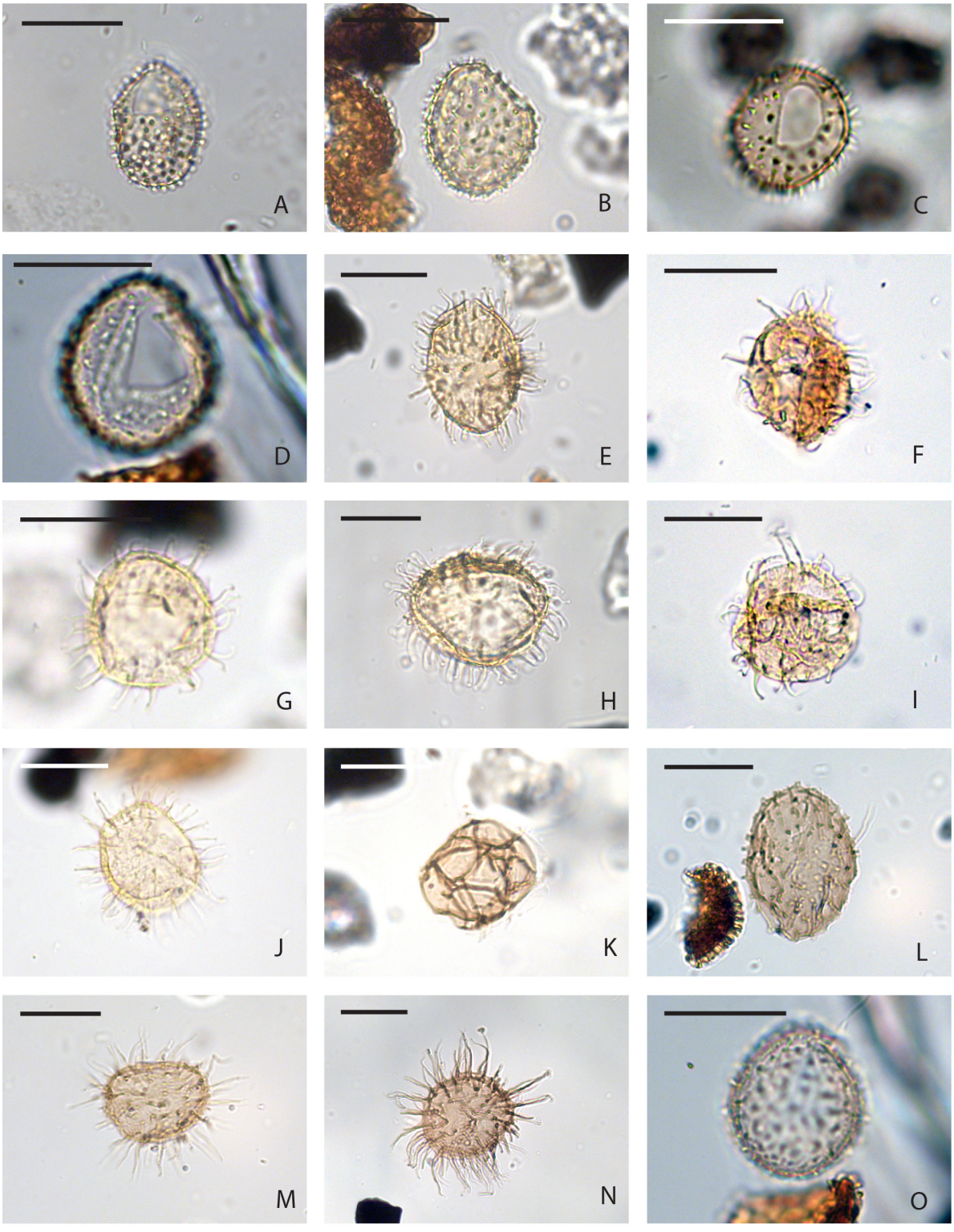

Plate 8. **(A)** *Operculodinium piaseckii*, Integrated Ocean Drilling Program Hole U1356A, Core 47R, Section 4W, interval 85–89 cm; **(B–D)** *Operculodinium janduchenei* 55R-1W, 9–13 cm. **(C)** 40R-2W, 9–22 cm; **(D)** 40R-2W, 19–22 cm; **(E–J)** *Operculodinium eirikianum* **(E)** 84R-4W, 120–124 cm; **(F)** 85R-5W, 39–43 cm; **(G)** 85R-4W, 60–64 cm; **(H)** 58R-1W, 19–23 cm; **(I)** 85R-5W, 39–43 cm; **(J)** 85R-5W, 100–104 cm; **(K)** *Protoperidinium* sp. D 58R-1W, 19–23 cm; **(L–M)** *Protoperidinium* sp. A **(L)** 88R-1W, 61–65 cm; **(M)** 84R-4W, 39–43 cm; **(N)** 93R-3W, 44–48 cm; **(O)** *Pyxidinopsis* sp. A 40R-2W, 19–21 cm. Scale bar is 25 µm.

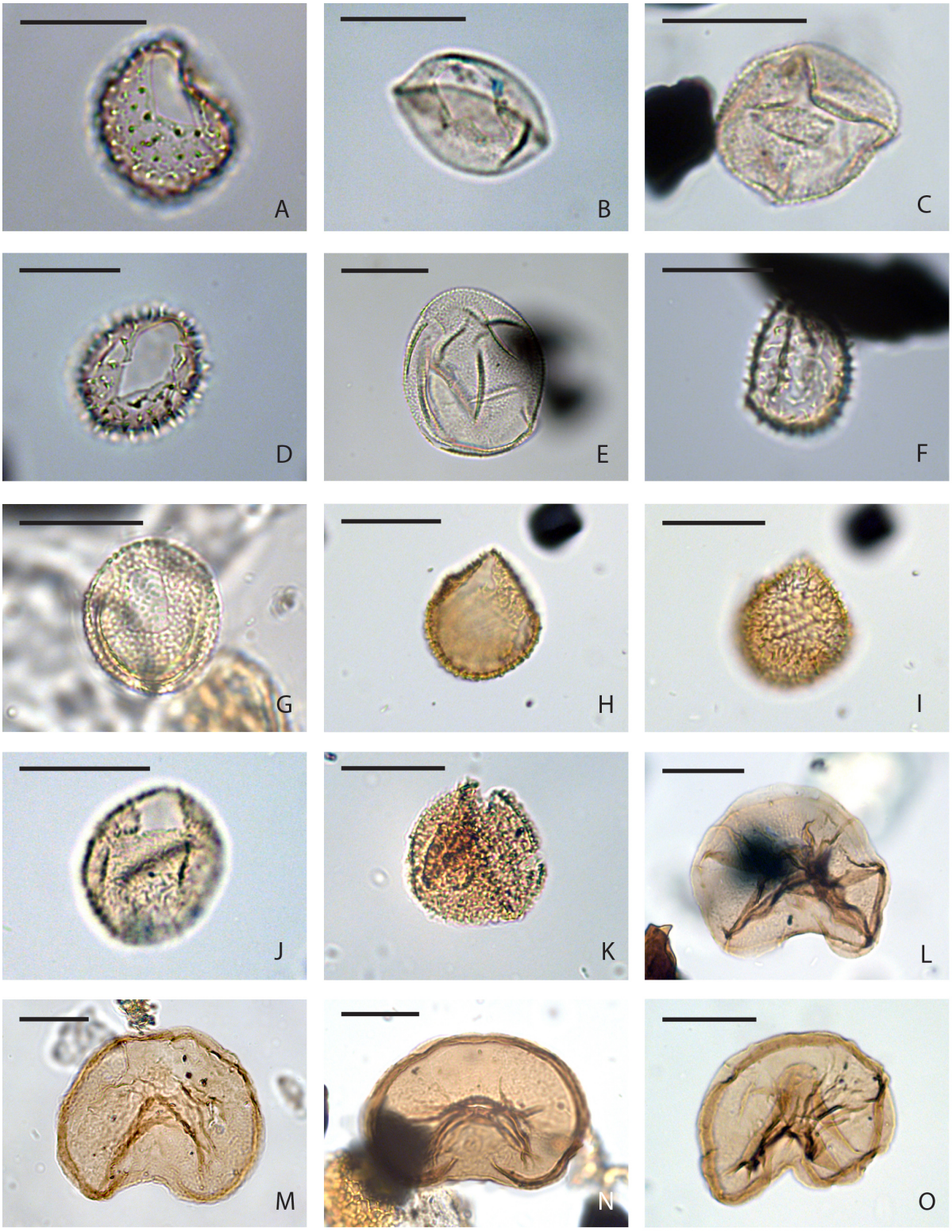

Plate 9. **(A)** *Pyxidinopsis* sp., Integrated Ocean Drilling Program Hole U1356A, Core 19R, Section 2W, interval 20–22 cm; **(B)** *Pyxidinopsis* sp. 19R-2W, 20–22 cm; **(C)** *Pyxidinopsis vesiculata* 17R-3W, 20–22 cm; **(D)** *Pyxidinopsis* sp. 34R-1W, 27–29 cm; **(E)** *Pyxidinopsis* sp. 30R-6W, 20–22 cm. **(F)** *Pyxidinopsis* sp. 19R-2W, 19–23 cm; **(G)** *Pyxidinopsis* sp. 46R-1W, 68–72 cm; **(H–K)** *Pyxidinopsis* sp. B **(H, I)** 84R-6W, 0–4 cm; **(J)** 85R-5W, 100–104 cm; **(K)** 87R-3W, 40–44 cm; **(L, M)** *Selenopemphix antarctica* **(L)** 85R-5W, 80–84 cm; **(M)** 94R-4W, 4–8 cm; **(N, O)** *Selenopemphix nephroides* **(N)** 84R-5W, 0–4 cm; **(O)** 84R-5W, 100–104 cm. Scale bar is 25 µm.

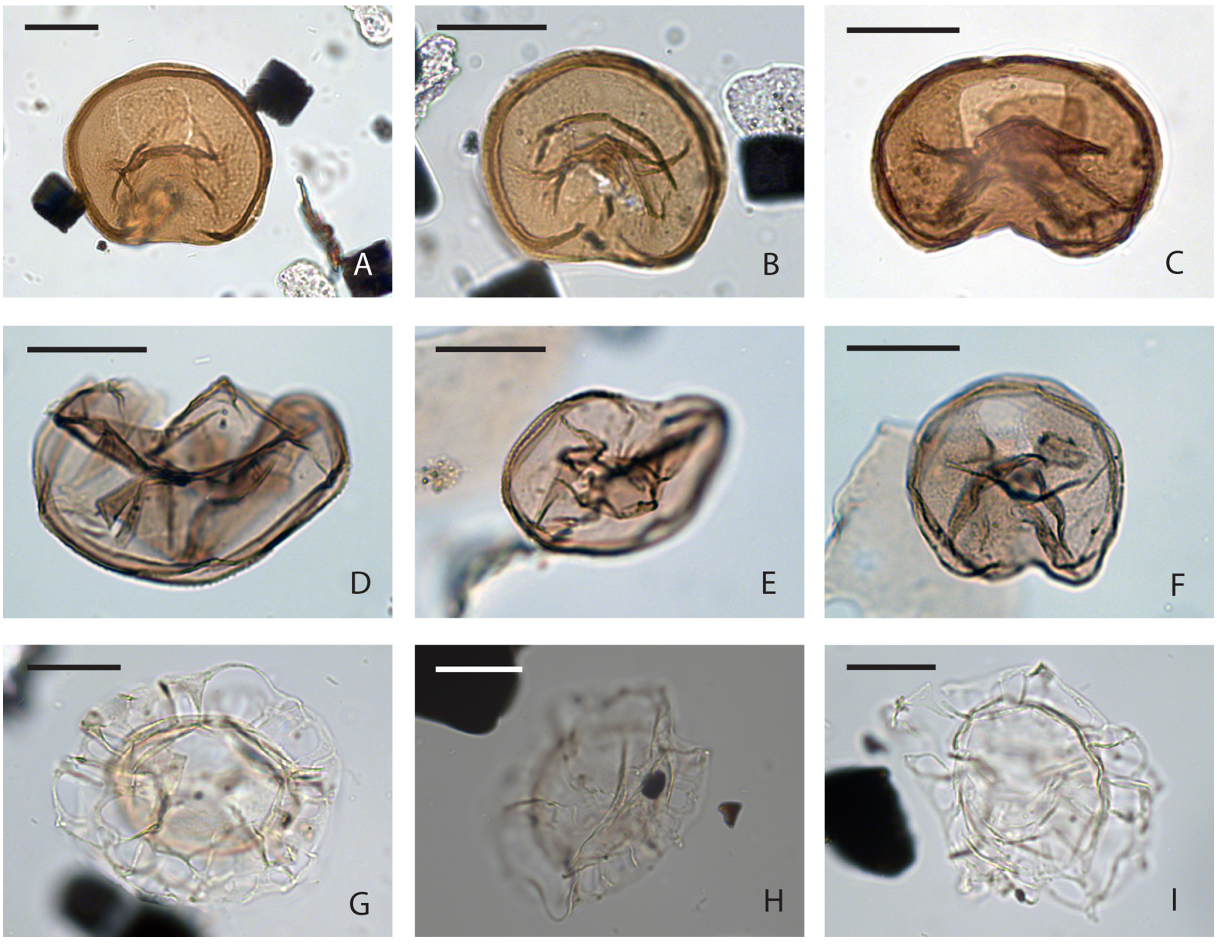

Plate 10. **(A)** *Selenopemphix nephroides*, Integrated Ocean Drilling Program Hole U1356A, Core 89R, Section 2W, interval 39–43 cm; **(B)** *Selenopemphix nephroides* 89R-2W, 39–43 cm; **(C)** *Selenopemphix nephroides* 95R-1W, 64–68 cm; **(D–F)** *Selenopemphix undulata* **(D)** 17R-3W, 20–22 cm; **(E)** 17R-1W, 20–22 cm; **(F)** 17R-3W, 20–22 cm; **(G–I)** *Unipontidinium aquaeductum* **(G)** 19R-5W, 20–22 cm; **(H)** 19R-5W, 20–22 cm; **(I)** 19R-5W, 20–22 cm. Scale bar is 25 µm.

Significant events. The LO of *Elytrocysta* spp., *Impagidinium victorianum*, *Protoperidinium* sp. B and sp. D, *I. velorum, Batiacasphaera* sp. C, *Operculodinium* cf. *eirikianum, Corrudinium labradori, Cleistosphaeridium* sp. B, and *Cerebrocysta* sp. A are found in this zone. The FOs of *I. elongatum* and cf. *Pyxidinopsis reticulata* are reported in this zone. Acritarchs are common throughout.

5.2.10 Zone SODZ10

Base definition. The base of this zone is defined by the FO of *Edwardsiella sexispinosa*.

Top definition. The top of this zone is defined by the base of SMDZ1, i.e. the FO of *Pyxidinopsis fairhavenensis*.

Type locality. IODP Site U1356.

Base sample. U1356A, 47R-1W, 45–49 cm (440.87 m b.s.f.).

Top sample. U1356A, 45R-1W, 10–14 cm (421.31 m b.s.f.).

Calibration. The base of this zone is calibrated to 80 % in C6Cn.2r. The top of this zone is calibrated to 80 % in C5Cr.

Age. 23.0–17.1 Ma. The time interval represented in the hiatus is discussed above, under Sect. 4.2. We chose to have this zone encompass the early Miocene hiatus in the type section. We hope that other sedimentary records can provide a more complete early Miocene sedimentary record by which zonations for this time interval can be proposed in order to improve the dinocyst zonation scheme.

Characteristic species. *Brigantedinium* spp., *Operculodinium* spp., *Batiacasphaera* spp., *Nematosphaeropsis labyrinthus* and *Impagidinium* spp.

Significant events. This zone contains the FOs of *Batiacasphaera sphaerica, Pyxidinopsis fairhavenensis,*

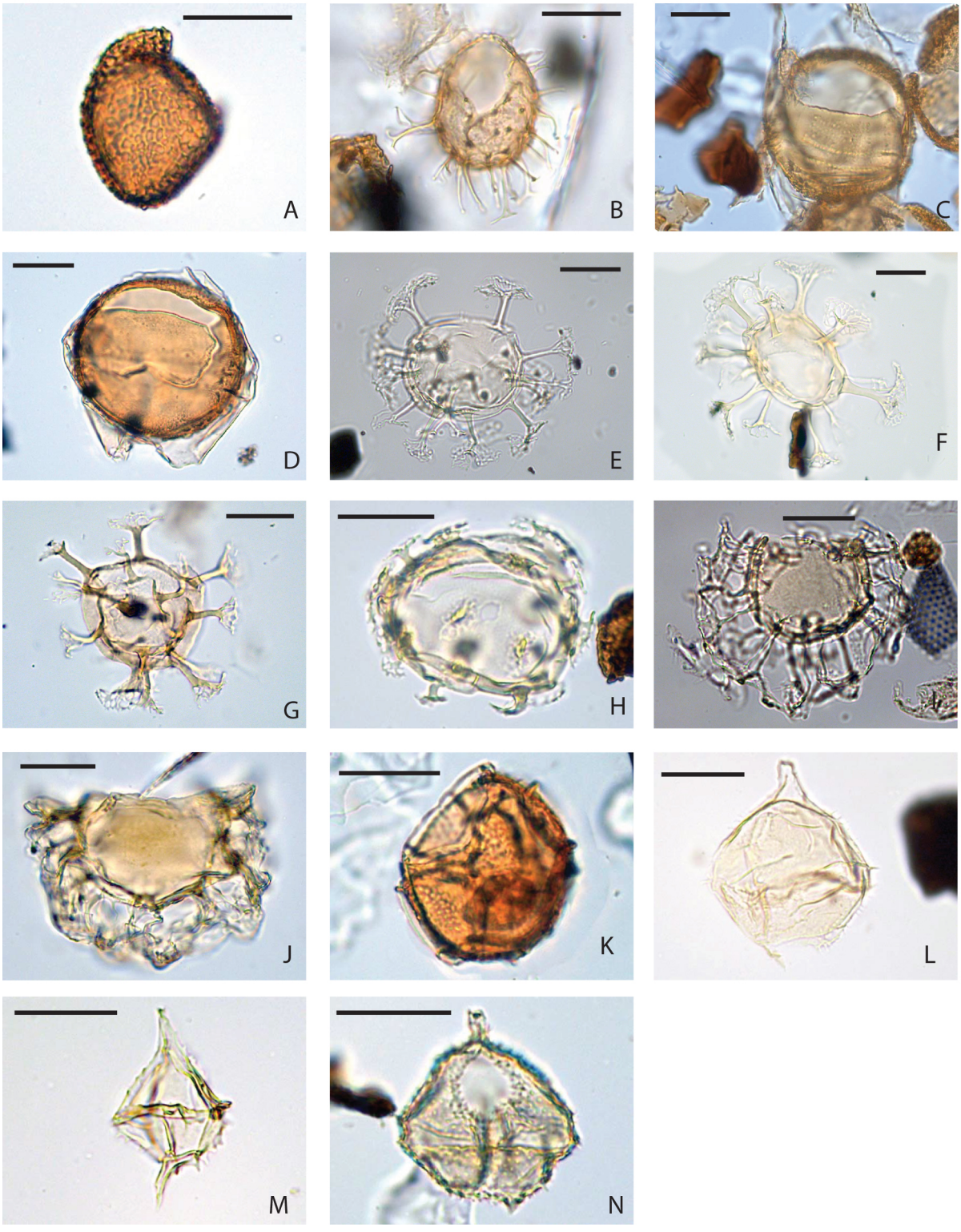

Plate 11. **(A)** *Cerebrocysta bartonensis*, Integrated Ocean Drilling Program Hole U1356A, Core 94R, Section 4W, interval 44–48 cm; **(B)** *Cleistosphaeridium diversispinosum* 94R-1W, 12–16 cm; **(C)** *Deflandrea antarctica* 94R-1W, 12–16 cm **(D)** *Deflandrea phosphoritica* 94R-4W, 44–48 cm; **(E–G)** *Enneadocysta dictyostila* **(E)** 86R-4W, 40–44 cm; **(F)** 85R-5W, 100–104 cm; **(G)** 85R-5W, 100–104 cm; **(H)** *Enneadocysta diktyostila* subsp. *Enneadostila brevistila* 94R-1W, 12–16 cm; **(I)** *Glaphyrocysta retiintexta* 94R-1W, 144–148 cm; **(J)** *Glaphyrocysta* sp. 94R-4W, 44–48 cm; **(K)** *Impagidinium maculatum* 94R-3W, 44–48 cm; **(L)** *Spinidinium macmurdoense* 94R-3W, 44–48 cm; **(M)** *Spinidinium schellenbergii* 94R-2W, 40–44 cm; **(N)** *Vozzhennikovia apertura* 94R-3W, 44–48 cm. Scale bar is 25 µm.

Cordosphaeridium minutum, Impagidinium cantabrigiense, Selenopemphix undulata, and *Brigantedinium* sp. B, sp. C and sp. D.

5.2.11 Zone SMDZ1

Base definition. The base of this zone is defined by the FO of *Pyxidinopsis fairhavenensis*.

Top definition. The top of this zone is defined by the base of SMDZ2, i.e. the LO of *Invertocysta tabulata*.

Type locality. IODP Site U1356.

Base sample. U1356A, 44R-1W, 20–24 cm (411.81 m b.s.f.).

Top sample. U1356A, 40R-2W, 19–21 cm (374.9 m b.s.f.).

Calibration. The base of this zone is calibrated to 80% in C5Cr. The top of this zone is calibrated to the top of C5Cn.2n.

Age. 17.1–16.3 Ma.

Characteristic species. *Operculodinium* spp., *Batiacasphaera* spp., *Nematosphaeropsis labyrinthus* and *Impagidinium* spp.

Significant events. This zone contains the (regional) LO of *Impagidinium elongatum* and *I. plicatum*. It includes the FO of *Operculodinium piaseckii*.

5.2.12 Zone SMDZ2

Base definition. The base of this zone is defined by the LOs of *Invertocysta tabulata*.

Top definition. The top of this zone is defined by the base of SMDZ3, i.e. the FO of *Unipontidinium aquaeductum*.

Type locality. IODP Site U1356.

Base sample. U1356A, 39R-1W, 20–22 cm (363.81 m b.s.f.).

Top sample. U1356A, 30R-6W, 20–22 cm (284.61 m b.s.f.).

Calibration. The base of this zone is calibrated to the base of C5Cn.2n. The top of this zone is calibrated to 75 % in C5Bn.2n.

Age. 16.5–15.1 Ma.

Characteristic species. *Brigantedinium pynei, Operculodinium janduchenei, Batiacasphaera* spp. and *Pyxidinopsis* spp.

Significant events. This zone sees the LOs of *Invertocysta tabulata* and *Impagidinium* sp. B and the FOs of *Habibacysta*? sp., *Selenopemphix* sp. A and *Cryodinium*? sp.

5.2.13 Zone SMDZ3

Base definition. The base of this zone is defined by the FO of *Unipontidinium aquaeductum*.

Top definition. The top of this zone is undefined.

Type locality. IODP Site U1356.

Base sample. U1356A, 30R-4W, 20–22 cm (282.21 m b.s.f.).

Top sample. Undefined.

Calibration. The base of this zone is calibrated to 75 % in C5Bn.2n. The top of this zone is calibrated to 33 % between the FO of the diatom species *Actinomma golowini* and the FO of *Denticulopsis praedimorpha*, in the absence of a proper paleomagnetic signal in the core (Tauxe et al., 2012).

Age. 15.1 Ma to an undefined end age.

Characteristic species. This zone is characterised by alternating high abundances of the combination of *Brigantedinium* spp. with *Selenopemphix* spp. and *Nematosphaeropsis labyrinthus* with *Operculodinium* spp. Towards the top of this zone, a high abundance of *Brigantedinium simplex*, *B. pynei* and *Selenopemphix nephroides* is observed.

Significant events. This zone sees the regional LO of *Reticulatosphaera actinocoronata*, an acme of *Palaeocystodinium golzowense* (at 14 Ma), *Impagidinium aculeatum, Lejeunecysta attenuata*, *Pyxidinopsis fairhavenensis,* and *Unipontidinium aquaeductum*, and the FOs of ?*Ataxiodinium choane* and *Batiacasphaera micropapillata*. There is a single occurrence of *Hystrichosphaeropsis obscura* at the base of the zone. This zone encompasses the LO of *Protoperidinium* sp. A, *Impagidinium patulum, Brigantedinium pynei, Cordosphaeridium minutum*, *Selenopemphix* sp. A, *Protoperidinium* sp. A, *S. undulata, Brigantedinium* sp. C, *Cryodinium* spp., and *Batiacasphaera micropapillata*, and includes the range of *I. cantabrigiense* and *Lejeunecysta cowiei* and contains one occurrence of *S. dionaeacysta.*

Table 6. Selected dinocyst species found in the present study, which have well-calibrated events elsewhere that are broadly consistent with their range at U1356.

	Species	Stratigraphic calibration in U1356A	Age (Ma)	Calibrated elsewhere	Age (Ma)	By	In
LO	*Batiacasphaera micropapillata*	100 % in C5ABn	13.0–11.0	0 % in CN5b	11.9	McMinn (1992)	Australia
FO	*Batiacasphaera minuta*	100 % in C6Cn.1n	22.564	50 % in Burdigalian	18.205	Bujak and Matsuoka (1986)	N Pacific Ocean
FO	*Edwardsiella sexispinosa*	C6Cn	23	C6Br?	22.4	Brinkhuis et al. (2003a)	Tasmania
				50 % in NP25	25	Versteegh and Zevenboom (1995)	Italy
FO	*Impagidinium japonicum*	< 11	10.8	0 % in Tortonian	11.8	Zegarra and Helenes (2011)	C Pacific Ocean
FO	*Invertocysta tabulata*	67 % in C6Cr	23.5	33 % in P22	25.8	Powell (1992)	North Sea
FO	*Operculodinium piasecki*	100 % in c6cn.3n	23.2	100 % C6AAn	21.2	Zevenboom (1995)	Italy
FO	*Oligokolpoma galeottii*	25 % in C12n	30.9	0 % in C12n	31	Pross et al. (2012)	Italy
LO	*Phthanoperidinium amoenum*	80 % in C12n	30.7	50 % in NP23	30.8	Powell (1992)	North Sea
FO	*Pyxidinopsis vesciculata*	C6Cn	23	C6An	20.1	Montanari et al. (1997)	Italy
FO	*Pyxidinopsis reticulata*	0 % in C5Cn	16.7	75 % in Burdigalian	17.1	Zegarra and Helenes, 2011	C Pacific Ocean
FO	*Selenopemphix dionea-cysta*	50 % in C5ABn	13.5	20 % in NN6	13.2	De Verteuil and Norris (1996)	
LO	*Stoveracysta ornata*	50 % in C12n	30.8	50 % in C12r	32.2	Brinkhuis et al. (2003a)	Tasmania
LO	*Stoveracysta kakanuiensis*	75 % in C13n	33.3	50 % in C12r	32.2	Brinkhuis et al. (2003a)	Tasmania
FO	*Unipontidinium aquae-ductum*	50 % in C5Bn	15	50 % in C5Bn.1r	15	Schreck et al. (2012)	N Atlantic Ocean
LO	*Unipontidinium aquae-ductum*	0 % C5ABn	13.6	0 % in C5An.2n	12.5	Zevenboom (1995)	Italy
				100 % in NN5	13.5	Schreck et al. (2012)	N Atlantic
ACME	*Palaeocystodinium golsowense*	50 % C5ACn	13.7	50 % in C5ACn	13.8	Quaijtaal et al. (2014)	N Atlantic

5.3 Correlation of stratigraphic ranges of selected non-endemic dinocysts

Although the majority of dinocyst taxa we find in our record comprise species that are endemic to the Southern Ocean, or are long-ranging and cosmopolitan, some species have well-calibrated stratigraphic ranges elsewhere. We list a selection of these species in Table 6. The consistency between our dinocyst stratigraphy and those of others lends some support to our dinocyst zonation and ties our zonation at least to some extent to other dinocyst stratigraphies. However, we are unable to tie our dinocyst events very precisely to other stratigraphies because many magnetic reversals in the record at U1356 fall within core gaps, which make the interpretation of magnetic reversals uncertain, and therewith, the position of the dinocyst events with respect to the magnetostratigraphy. Moreover, comparison of dinocyst events across latitudes has proven complicated because dinocysts tend to be very sensitive to environmental conditions, which may not necessarily change in tandem over the globe through time. Therefore, dinocysts generally tend to have asynchronous originations and extinctions across different latitudinal bands over the globe (e.g. Williams et al., 2004). Nonetheless, with an error bar of about 200 kyr, some dinocyst events (Table 6) seem to be consistent between Site U1356 and a variety of locations over the globe, which adds to their significance as a biostratigraphic marker, and may help to stratigraphically date sediments from other parts of the Southern Ocean as well.

6 Conclusions

We formally describe two new dinoflagellate cyst species and present a first zonation scheme for Oligocene–Miocene dinocysts of the Southern Ocean. Temporal resolution of the proposed zonation is in some intervals sufficiently high to allow accurate (i.e. ca. 500 kyr resolution) stratigraphic calibration. However, in some intervals, poor core recovery, two hiatuses covering the early Miocene (~ 23.0–17.1 Ma) and the middle Miocene (~ 13.4–11 Ma) and/or low species diversity cause zones with an undesirably long duration. We acknowledge that the zonation might not be applicable to all dinocyst-bearing Southern Ocean sediments due to the strong

(latitudinal) provincialism of the dinocyst biogeography in the Southern Ocean today.

Data availability. Data are available at https://doi.pangaea.de/10.1594/PANGAEA.883747 (Bijl et al., 2017).

Author contributions. PKB, FS and JP designed the research. AJPH, PKB, AB and FS carried out dinocyst analyses for the earliest Oligocene, the mid- to upper Oligocene, the Oligocene–Miocene boundary and the Miocene respectively. PKB integrated, cross-validated and compiled the data and wrote the paper with input from all co-authors.

Competing interests. The authors declare that they have no conflict of interest.

Acknowledgements. We thank the constructive reviews of Michael J. Hannah and Kasia S. Śliwińska, which really improved our paper. This research used samples and data from the Integrated Ocean Drilling Program. IODP was sponsored by the US National Science Foundation and participating countries under management of Joined Oceanographic Institutions Inc. PKB and FS thank NWO-NNPP grant no. 866.10.110, NWO-ALW VENI grant no. 863.13.002 for funding and Natasja Welters for technical support. We thank Margot Cramwinckel for producing the illustrations in Fig. 5.

Edited by: Luke Mander
Reviewed by: Michael Hannah and Kasia K. Sliwinska

References

Artzner, D. G. and Dörhöfer, G.: Taxonomic note: *Lejeunecysta* nom. nov. pro Lejeunia Gerlanch 1961 emend Lentin and Williams, 1976 – dinoflagellate cyst genus, Can. J. Botany, 56, 1381–1382, 1978.

Benedek, P. N.: Phytoplanktonten aus dem Mittel- und Oberoligozän von Tonisberg (Niederrheingebiet), Paleontographica, Abteilung B, 137, 1–71, 1972.

Bijl, P. K., Houben, A. J. P., Schouten, S., Bohaty, S. M., Sluijs, A., Reichart, G. J., Sinninghe Damsté, J. S., and Brinkhuis, H.: Transient Middle Eocene Atmospheric Carbon Dioxide and Temperature Variations, Science, 330, 819–821, 2010.

Bijl, P. K., Pross, J., Warnaar, J., Stickley, C.E., Huber, M., Guerstein, R., Houben, A.J.P., Sluijs, A., Visscher, H., and Brinkhuis, H.: Environmental forcings of Paleogene Southern Ocean dinoflagellate biogeography, Paleoceanography, 26, PA1202, https://doi.org/10.1029/2009PA001905, 2011.

Bijl, P. K., Bendle, A. P. J., Bohaty, S. M., Pross, J., Schouten, S., Tauxe, L., Stickley, C. E., McKay, R. M., Röhl, U., Olney, M., Sluijs, A., Escutia, C., Brinkhuis, H., and Expedition 318 scientists: Eocene cooling linked to early flow across the Tasmanian Gateway, P. Natl. Acad. Sci. USA, 110, 9645–9650, 2013a.

Bijl, P. K., Sluijs, A., and Brinkhuis, H.: A magneto- chemostratigraphically calibrated dinoflagellate cyst zonation of the early Paleogene South Pacific Ocean, Earth-Sci. Rev., 124, 1–31, 2013b.

Bijl, P. K., Sluijs, A., and Brinkhuis, H.: Erratum to "A magneto- and chemostratigraphically calibrated dinoflagellate cyst zonation of the early Paleogene South Pacific Ocean" (Earth Sci. Rev., 124, 1–31, 2013), Earth-Sci. Rev., 134, 160–163, 2014.

Bijl, P. K., Brinkhuis, H., Egger, L. M., Eldrett, J. S., Frieling, J., Grothe, A., Houben, A. J. P., Pross, J., Sliwinska, K. K., and Sluijs, A.: Comment on "*Wetzeliella* and its allies – the "hole" story: a taxonomic revision of the Paleogene dinoflagellate subfamily Wetzelielloideae" by Williams et al. (2015), Palynology, 41, 423–429, 2016.

Bijl, P. K., Houben, A. J. P., Bruls, A., Pross, J., Sangiorgi, F., García-Alix, A.: Dinoflagellate cysts in the Oligocene to Miocene sediments of IODP Site 318-U1356A, PANGAEA, https://doi.org/10.1594/PANGAEA.883747, 2017.

Brinkhuis, H., Munsterman, D. M., Sengers, S., Sluijs, A., Warnaar, J., and Williams, G. L.: Late Eocene to Quaternary dinoflagellate cysts from ODP Site 1168, off western Tasmania, in: Proceedings of the Ocean Drilling Program, Scientific Results, edited by: Exon, N. and Kennett, J. P., Vol. 189, U.S. Government Printing Office, College Station, Texas, 2003a.

Brinkhuis, H., Sengers, S., Sluijs, A., Warnaar, J., and Williams, G. L.: Latest Cretaceous to earliest Oligocene, and Quaternary dinoflagellates from ODP Site 1172, East Tasman Plateau, in: Proceedings of the Ocean Drilling Program, Scientific Results, edited by: Exon, N. and Kennett, J. P., Vol. 189, U.S. Government Printing Office, College Station, Texas, 2003b.

Bujak, J. P. and Davies, E. H.: Modern and fossil Peridiniineae, American Association of Stratigraphic Palynologists Foundation Contr. Series, 13, 1–212, 1983.

Bujak, J. P. and Matsuoka, K.: Late Cenozoic dinoflagellate cyst zonation in the western and Northern Pacific, AASP Contributions Series, 17, 7–25, 1986.

Bujak, J. P., Downie, C., Eaton, G. L., and Williams, G. L.: Dinoflagellate cysts and acritarchs from the Eocene of southern England, Special Papers in Paleontology, 24, 100 pp., 1980.

Bütschli, O.: Erster Band. Protozoa, in: Dr. H. G. Bronnes Klassen und Ordnungen des Thier-Reichs, wissenschaftlich dargestellt in Wort und Bild, edited by: Bronn, H. G., C. F. Winter'sche Verlagsbuchhandlung, Leipzig und Heidelberg, 865–1088, 1885.

Clowes, C. D., Hannah, M. J., Wilson, G. J., and Wrenn, J. H.: Marine palynostratigraphy and new species from the Cape Roberts Drill-holes, Victoria Land Basin, Antarctica, Mar. Micropaleontol., 126, 65–84, 2016.

Cody, R. D., Levy, R. H., Harwood, D. M., and Sadler, P. M.: Thinking outside the zone: High-resolution quantitative diatom biochronology for the Antarctic Neogene, Palaeogeogr. Palaeocl., 260, 92–121, 2008.

Coxall, H. K. and Wilson, P. A.: Early Oligocene glaciation and productivity in the eastern equatorial Pacific: Insights into global carbon cycling, Paleoceanography, 26, PA2221, https://doi.org/10.1029/2010PA002021, 2011.

Crampton, J. S., Cody, R. D., Levy, R., Harwood, D., McKay, R., and Naish, T. R.: Southern Ocean phytoplankton turnover in response to stepwise Antarctic cooling over the past 15 million years, P. Natl. Acad. Sci. USA, 113, 6868–6873, 2016.

DeMaster, D. J.: The Diagenesis of Biogenic Silica: Chemical Transformations Occurring in the Water Column, Seabed, and Crust, Treatise on Geochemistry, 7, 87–98, 2003.

de Verteuil, L. and Norris, G.: Miocene dinoflagellate stratigraphy and systematics of Maryland and Virginia, Micropaleontology, 42, 1–172, 1996.

Egger, L. M., Sliwinska, K. K., van Peer, T. E., Liebrand, D., Lippert, P. C., Friedrich, O., Wilson, P. A., Norris, R. D., and Pross, J.: Magnetostratigraphically-calibrated dinoflagellate cyst bioevents for the uppermost Eocene to lowermost Miocene of the western North Atlantic (IODP Expedition 342, Paleogene Newfoundland sediment drifts), Rev. Palaeobot. Palyno., 234, 159–185, 2016.

Eldrett, J. S., Harding, I. C., Firth, J. V., and Roberts, A. P.: Magnetostratigraphic calibration of Eocene-Oligocene dinoflagellate cyst biostratigraphy from the Norwegian-Greenland Sea, Mar. Geol., 204, 91–127, 2004.

Escutia, C., Brinkhuis, H., Klaus, A., and Expedition 318 Scientists: Proceedings of the Integrated Ocean Drilling Program, Initial Results, Vol. 318, Integrated Ocean Drilling Program Management International, Inc., Tokyo, 2011.

Evitt, W. R.: Sporopollenin dinoflagellate cysts. Their morphology and interpretation, American Association of Stratigraphic Palynology Foundation, Austin, TX, 1985.

Fensome, R. A., Taylor, F. J. R., Norris, G., Sarjeant, W. A. S., Wharton, D. I., and Williams, G. L.: A Classification of Modern and Fossil Dinoflagellates, Micropaleontology, Special publication number 7, American Museum of Natural History, Salem, USA, 1993.

Goodman, D. K. and Ford Jr., L. N.: Preliminary dinoflagellate biostratigraphy for the middle Eocene to Lower Oligocene from the Southwest Altantic Ocean, edited by: Ludwig, W. J., Krasheninnikov, V. A., and Wise Jr., W. S., Initial Reports of the Deep Sea Drilling Project, Vol. 71, https://doi.org/10.2973/dsdp.proc.71.131.1983, Washington, U.S., Govternment Printing Office 859–977, 1983.

Gradstein, F. M., Ogg, J. G., and Smith, A. G.: A geologic timescale 2004, Cambridge University Press, Cambridge, 2004.

Gradstein, F. M., Ogg, J. G., Schmitz, M. D., and Ogg, G. M.: The Geologic Time Scale 2012, The Geologic Time Scale 2012, 2, 437–1144, 2012.

Haeckel, E.: Systematische Phylogenie. Entwurf eines naturlichen Systems der Organismen auf Grund ihrer Stammegeschichte, I., in: Anonymous Systematische Phylogenie der Protisten und Pflanzen, Reimer, Berlin, XV+400, 1984.

Hannah, M. J.: Eocene dinoflagellates from CIROS-1 drill hole, McMurdo Sound, Antarctica, Terra Antarctica, 1, p. 371, 1994.

Hannah, M. J.: Climate controlled dinoflagellate distribution in late Eocene – earliest Oligocene strata from CIROS-1 drillhole, McMurdo Sound, Antarctica, Terra Antarctica, 4, 73–78, 1997.

Hannah, M. J.: The palynology of ODP Site 1165, Prydz Bay, East Antarctica: A record of Miocene glacial advance and retreat, Palaeogeogr. Palaeocl., 231, 120–133, 2006.

Hannah, M. J., Wrenn, J. H., and Wilson, G. L.: Early Miocene and quaternary marine palynomorphs from Cape Roberts Project CRP-1, McMurdo Sound, Antarctica, Terra Antarctica, 5, 527–538, 1998.

Hannah, M. J., Wilson, G. J., Wrenn, and J. H.: Oligocene and miocene marine palynomorphs from CRP-2/2A, Victoria Land Basin, Antarctica, Terra Antarctica, 7, 503–511, 2000.

Hannah, M. J., Florindo, F., Harwood, D. M., and Fielding, C. R.: Chronostratigraphy of the CRP-3 drillhole, Victoria Land Basin, Antarctica, Terra Antarctica, 8, 615–620, 2001a.

Hannah, M. J., Wrenn, J. H., and Wilson, G. J.: Preliminary report on early Oligocene and ?latest Eocene marine palynomorphs from CRP-3 drillhole, Victoria Land Basin, Antarctica, Terra Antarctica, 8, 383–388, 2001b.

Head, M. J.: Morphology and paleoenvironmental significance of the Cenozoic dinoflagellate genera Tectatodinium and Habibacysta, Micropaleontology, 40, 289–321, 1994.

Houben, A. J. P., Bijl, P. K., Guerstein, G. R., Sluijs, A., and Brinkhuis, H.: *Malvinia escutiana*, a new biostratigraphically important Oligocene dinoflagellate cyst from the Southern Ocean, Rev. Palaeobot. Palyno., 165, 175, 2011.

Houben, A. J. P., van Mourik, C. A., Montanari, A., Coccioni, R., and Brinkhuis, H.: The Eocene-Oligocene transition: Changes in sea level, temperature or both?, Palaeogeogr. Palaeocl., 335–336, 75–83, 2012.

Houben, A. J. P., Bijl, P. K., Pross, J., Bohaty, S. M., Passchier, S., Stickley, C. E., Röhl, U., Sugisaki, S., Tauxe, L., Van De Flierdt, T., Olney, M., Sangiorgi, F., Sluijs, A., Escutia, C., and Brinkhuis, H.: Reorganization of Southern Ocean plankton ecosystem at the onset of Antarctic glaciation, Science, 340, 341–344, 2013.

Juggins, S.: C2 Version 1.5 User guide, Software for ecological and palaeoecological data analysis and visualisation, Newcastle University, Newcastle upon Tyne, UK, 2007.

McKay, R. M., Barrett, P. J., Levy, R. S., Naish, T. R., Golledge, N. R., and Pyne, A.: Antarctic Cenozoic climate history from sedimentary records: ANDRILL and beyond, Philos. T. R. Soc. A, 374, 20140301, https://doi.org/10.1098/rsta.2014.0301, 2016.

McMinn, A.: Neogene dinoflagellate distribution in the eastern Indian Ocean from Leg 123, Site 765, in: Proc. ODP, Sci. Results 123, edited by: Gradstein, F. M., Adamseon, A. C., Ludden, J. N., and Poag, C. W., Ocean Drilling Program, College Station, TX, 429–441, https://doi.org/10.2973/odp.proc.sr.123.120.1992, 1992.

Mertens, K. N., Takano, Y., Head, M. J., and Matsuoka, K.: Living fossils in the Indo-Pacific warm pool: A refuge for thermophilic dinoflagellates during glaciations, Geology, 42, 531–534, 2014.

Montanari, A., Bice, D. M., Capo, R., Coccioni, R., Deino, A., DePaolo, D. J., Emmanuel, L., Monechi, S., Renard, M., and Zevenboom, D.: Integrated stratigraphy of the Chattian to mid-Burdigalian pelagic sequence of the Contessa Valley (Gubbio, Italy), in: Miocene Stratigraphy: an Integrated Approach, edited by: Montanari, A., Odin, G. S., and Coccioni, R., Elsevier Science B.V., Amsterdam, the Netherlands, 1997.

Pälike, H., Norris, R. D., Herrle, J. O., Wilson, P. A., Coxall, H. K., Lear, C. H., Shackleton, N. J., Tripati, A. K., and Wade, B. S.: The Heartbeat of the Oligocene Climate System, Science, 314, 1894–1898, 2006.

Pascher, A.: Uber Flagellaten und Algen, Deutsche Botanische Gesellschaft, Berichte, 32, 136–160, 1914.

Powell, A. J.: A Stratigraphic Index of Dinoflagellate Cysts, Chapman and Hall, London, 1992.

Prebble, J. G., Crouch, E. M., Carter, L., Cortese, G., Bostock, H., and Neil, H.: An expanded modern dinoflagellate cyst dataset for the Southwest Pacific and Southern Hemisphere with environmental associations, Mar. Micropaleontol., 101, 33–48, 2013.

Pross, J., Houben, A. J. P., Simaeys, S. v., Williams, G. L., Kotthoff, U., Coccioni, R., Wilpshaar, M., and Brinkhuis, H.: Umbria-Marche revisited: A refined magnetostratigraphic calibration of dinoflagellate cyst events for the Oligocene of the Western Tethys, Rev. Palaeobot. Palyno., 158, 213–235, 2010.

Pross, J., Contreras, L., Bijl, P. K., Greenwood, D. R., Bohaty, S. M., Schouten, S., Bendle, J. A., Röhl, U., Tauxe, L., Raine, I., Huck, C. E., van de Flierdt, T., Jamieson, S. S. R., Stickley, C. E., van de Schootbrugge, B., Escutia, C., Brinkhuis, H., and Expedition 318 Scientists: Persistent near-tropical warmth on the Antarctic continent during the early Eocene epoch, Nature, 488, 73–77, 2012.

Quaijtaal, W., Donders, T. H., Persico, D., and Louwye, S.: Characterising the middle Miocene Mi-events in the Eastern North Atlantic realm: A first high-resolution marine palynological record from the Porcupine Basin, Palaeogeogr. Palaeocl., 399, 140–159, 2014.

Sangiorgi, F., Bijl, P. K., Passchier, S., Salzmann, U., Schouten, S., Pross, J., Bohaty, S. M., McKay, R., van de Flierdt, T., Levy, R., Williams, T., Escutia, C., and Brinkhuis, H.: A warm Southern Ocean and retreated Wilkes Land ice sheet (East Antarctica) during the mid-Miocene, Nat. Commun., in press, 2017.

Schreck, M., Matthiessen, J., and Head, M. J.: A magnetostratigraphic calibration of Middle Miocene through Pliocene dinoflagellate cyst and acritarch events in the Iceland Sea (Ocean Drilling Program Hole 907A), Rev. Palaeobot. Palyno., 187, 66–94, 2012.

Seton, M., Müller, R. D., Zahirovic, S., Gaina, C., Torsvik, T., Shephard, G., Talsma, A., Gurnis, M., Turner, M., Maus, S., and Chandler, M.: Global continental and ocean basin reconstructions since 200 Ma, Earth-Sci. Rev., 113, 212–270, 2012.

Sluijs, A., Brinkhuis, H., Stickley, C. E., Warnaar, J., Williams, G. L., and Fuller, M.: Dinoflagellate cysts from the Eocene–Oligocene transition in the Southern Ocean: results from ODP Leg 189, in: Proceedings of the Ocean Drilling Program, edited by: Exon, N. and Kennett, J. P., Scientific Results, Vol. 189, U.S. Government Printing Office, College Station, Texas, 2003.

Sluijs, A., Schouten, S., Pagani, M., Woltering, M., Brinkhuis, H., Sinninghe Damsté, J. S., Dickens, G. R., Huber, M., Reichart, G., Stein, R., Matthiessen, J., Lourens, L. J., Pedentchouk, N., Backman, J., Moran, K., and Expedition 302 scientists: Subtropical Arctic Ocean temperatures during the Palaeocene/Eocene thermal maximum, Nature, 441, 610–613, 2006.

Stocchi, P., Escutia, C., Houben, A. J. P., Vermeersen, B. L. A., Bijl, P. K., Brinkhuis, H., DeConto, R. M., Galeotti, S., Passchier, S., Pollard, D., Klaus, A., Fehr, A., Williams, T., Bendle, J. A. P., Bohaty, S. M., Carr, S. A., Dunbar, R. B., Flores, J. A., Gonzàlez, J. J., Hayden, T. G., Iwai, M., Jimenez-Espejo, F. J., Katsuki, K., Kong, G. S., McKay, R. M., Nakai, M., Olney, M. P., Pekar, S. F., Pross, J., Riesselman, C., Röhl, U., Sakai, T., Shrivastava, P. K., Stickley, C. E., Sugisaki, S., Tauxe, L., Tuo, S., Van De Flierdt, T., Welsh, K., and Yamane, M.: Relative sea-level rise around East Antarctica during Oligocene glaciation, Nat. Geosci., 6, 380–384, 2013.

Tauxe, L., Stickley, C. E., Sugisaki, S., Bijl, P. K., Bohaty, S., Brinkhuis, H., Escutia, C., Flores, J. A., Iwai, M., Jimenez-Espejo, F., McKay, R., Passchier, S., Pross, J., Riesselman, C., Rohl, U., Sangiorgi, F., Welsh, K., Klaus, A., Bendle, J. A. P., Dunbar, R., Gonzalez, J., Olney, M. P., Pekar, S. F., van de Flierdt, T.: Chronostratigraphic framework for the IODP Expedition 318 cores from the Wilkes Land Margin: constraints for paleoceanographic reconstruction, Paleoceanography, 27, PA2214, https://doi.org/10.1029/2012PA002308, 2012.

Ter Braak, C. J. F.: Canonical Correspondence Analysis: A new eigenvector technique for multivariate direct gradient analysis, Ecology, 67, 1167–1179, 1986.

Torsvik, T. H., Van der Voo, R., Preeden, U., Niocaill, C. M., Steinberger, B., Doubrovine, P. V., van Hinsbergen, D. J. J., Domeier, M., Gaina, C., Tohver, E., Meert, J. G., McCausland, P. J., and Cocks, L. R. M.: Phanerozoic polar wander, palaeogeography and dynamics, Earth-Sci. Rev., 114, 325–368, 2012.

Truswell, E. M.: Palynology of seafloor samples collected by the 1911–1914 Australasian Antarctic expedition: Implications for the geology of coastal East Antarctica, J. Geol. Soc. Aust., 29, 343–356, 1982.

Van Hinsbergen, D. J. J., De Groot, L. V., Van Schaik, S. J., Spakman, W., Bijl, P. K., Sluijs, A., Langereis, C. G., and Brinkhuis, H.: A paleolatitude calculator for paleoclimate studies, PLoS ONE, 10, e0126946, https://doi.org/10.1371/journal.pone.0126946, 2015.

Versteegh, G. J. M. and Zevenboom, D.: New genera and species of dinoflagellate cysts from the Mediterranean Neogene, Rev. Palaeobot. Palyno., 85, 213–229, 1995.

Warnaar, J.: Climatological implications of Australian-Antarctic separation, LPP Contributions series no. 22, 2006.

Warnaar, J., Bijl, P. K., Huber, M., Sloan, L. C., Brinkhuis, H., Röhl, U., Sriver, R., and Visscher, H.: Orbitally forced climate changes in the Tasman sector during the Middle Eocene, Palaeogeogr. Palaeocl., 280, 361–370, 2009.

Warny, S., Askin, R. A., Hannah, M. J., Mohr, B. A. R., Raine, J. I., Harwood, D. M., and Florindo, F.: Palynomorphs from a sediment core reveal a sudden remarkably warm Antarctica during the middle Miocene, Geology, 37, 955–958, 2009.

Williams, G. L., Brinkhuis, H., Pearce, M. A., Fensome, R. A., and Weegink, J. W.: Southern Ocean and global dinoflagellate cyst events compared: Index events for the late Cretaceous – Neogene, in: Proceedings of the Ocean Drilling Program, edited by: Exon, N. F., Kennett, J. P., and Malone, M. J., Scientific Results, Vol. 189, 1–98, 2004.

Williams, G. L., Fensome, R. A., and MacRae, R. A.: The Lentin and Williams Index of Fossil Dinoflagellates 2017 Edition, AASP Contributions Series Number 48, Dallas, Texas, USA, 2017.

Zegarra, M. and Helenes, J.: Changes in Miocene through Pleistocene dinoflagellates from the Eastern Equatorial Pacific (ODP Site 1039), in relation to primary productivity, Mar. Micropaleontol., 81, 107–121, 2011.

Zevenboom, D.: Dinoflagellate cysts from the Mediterranean late Oligocene and Miocene, PhD thesis, Utrecht University, Utrecht, the Netherlands, 1995.

Zhang, Y. G., Pagani, M., Liu, Z., Bohaty, S. M., and Deconto, R.: A 40-million-year history of atmospheric CO_2, Philos. T. R. Soc. A, 371, 20130096, https://doi.org/10.1098/rsta.2013.0096, 2013.

Zonneveld, K. A. F., Marret, F., Versteegh, G. J. M., Bogus, K., Bonnet, S., Bouimetarhan, I., Crouch, E., de Vernal, A., Elshanawany, R., Edwards, L., Esper, O., Forke, S., Grøsfjeld, K., Henry, M., Holzwarth, U., Kielt, J., Kim, S., Ladouceur, S., Ledu, D., Chen, L., Limoges, A., Londeix, L., Lu, S., Mahmoud, M.S., Marino, G., Matsouka, K., Matthiessen, J., Mildenhal, D.C., Mudie, P., Neil, H.L., Pospelova, V., Qi, Y., Radi, T., Richerol, T., Rochon, A., Sangiorgi, F., Solignac, S., Turon, J., Verleye, T., Wang, Y., Wang, Z., and Young, M.: Atlas of modern dinoflagellate cyst distribution based on 2405 data points, Rev. Palaeobot. Palyno., 191, 1–197, 2013.